Manufacturing Rev. **9**, 27 (2022)
© B. Mallikarjuna, E.W. Reutzel, Published by EDP Sciences 2022
https://doi.org/10.1051/mfreview/2022024

**Special Issue – Advanced Manufacturing Research for Aeronautics**
**Pr. Costas A. Charitidis (Ed.)**

**Manufacturing Review**
Available online at:
https://mfr.edp-open.org

REVIEW OPEN ACCESS

# Reclamation of intermetallic titanium aluminide aero-engine components using directed energy deposition technology

Balichakra Mallikarjuna[1,*] and Edward W. Reutzel[2]

[1]Department of Mechanical Engineering, Amrita School of Engineering, Coimbatore, Amrita Vishwa Vidyapeetham, India
[2]Applied Research Laboratory, Pennsylvania State University, Pennsylvania, USA

Received: 11 January 2022 / Accepted: 4 August 2022

**Abstract.** Titanium Aluminide (TiAl) alloys are intermetallics that offer low density, high melting point, good oxidation and corrosion resistance compared to Ni-based superalloys. As a result, these alloys are used in aero-engine parts such as turbine blades, fuel injectors, radial diffusers, divergent flaps, and more. During operation, aero-engine components are subjected to high thermal loading in an oxidizing and corrosive environment, which results in wear and other material damage. Replacement of the entire component may not be desirable due to long lead time and expense. In such cases, repair and refurbishing may be the best option for the reclamation of TiAl parts. Unfortunately, approved repair technology is not currently available for TiAl based components. Additive Manufacturing (AM) based Directed Energy Deposition (DED) may serve as an option to help repair and restore expensive aero-engine parts. In this work, a review of efforts to utilize the DED technique to repair damaged TiAl-based aerospace parts locally is conducted. Replacing the entire TiAl part is not advisable as it is expensive. DED is a promising technique used to produce, repair, rework, and overhaul (MRO) damaged parts. Considering the high-quality standard of the aircraft industry, DED repaired TiAl parts to be certified for their future use in the aircraft is very important. However, there are no standards for the certification of TiAl repaired parts is reported. Case studies reveal that DED is under consideration for repair of TiAl parts. Hybrid technology comprising machining, repair and finishing capability in a single machine is an attractive implementation strategy to improve repair efficacies. The review shows that the investigations into development and applications of DED-based repairing techniques are limited, which suggests that further investigations are very much needed.

**Keywords:** Titanium aluminide / intermetallics / directed energy deposition / aero-engine / repair

## 1 Introduction

Titanium Aluminide (TiAl) alloys are intermetallics used in various sectors, including aerospace, automotive, military, space, due to numerous favourable intrinsic properties [1–3]. Table 1 presents the potential applications of TiAl alloys. Due to the low density, high specific strength, and good oxidation and corrosion resistance of TiAl [4,5], significant research is underway to investigate potential benefits of using the alloys in aero-engine parts such as turbine blades, fuel injectors, exotic parts, divergent flaps, and more [6,7]. TiAl is a frontrunner for replacing the existing Ni-based alloys in order to reduce the weight of gas turbine engines and improve performance [1,3,8]. Table 2 reports the properties of TiAl alloys compared to superalloys often used in aero-engine applications [6].

Several aero-engine parts are already built using TiAl, as the favourable mechanical properties lead to reduced fuel consumption and pollutant emissions in practice [1,6]. It is well known that every component has a lifespan for functioning, after which the component degrades and subsequently fails to perform as required. The aero-engine parts have to operate in highly oxidizing and corrosive environments and are subjected to high fatigue and creep cycles [20,21]. As a result, components wear and performance degrades over time. After being damaged or degraded, it is necessary to replace such components, and this can be expensive [22,23]. Therefore, repair or refurbishing of parts becomes an opportunity to reduce overall operational cost.

Researchers have employed various methods to repair aero-engine components, such as Powder Metallurgy (PM), welding (GTAW-Gas Tungsten Arc Welding, PAW-Plasma Arc Welding), High-Velocity Oxy-Fuel (HVOF), brazing, and plasma spray [24–29]. Ellison et al. used an advanced powder metallurgy technique known as Liburdi Powder Metallurgy (LPM) to repair and

* e-mail: mallubalichakra@gmail.com

**Table 1.** Potential applications of TiAl based alloys.

| Alloy | Important phase of alloy | Applications | Potential TiAl Components | References |
|---|---|---|---|---|
| γ-TiAl based alloys | γ-TiAl (hexagonal $DO_{19}$ structure) and $\alpha_2$-$Ti_3Al$ (tetragonal $L1_0$ structure) | Aerospace | Airframes | [9] |
| | | | Exhaust nozzle | [7] |
| | | | Divergent flap | [6,7] |
| | | | Side wall/sheet | [7] |
| | | | I-Beam | [7] |
| | | | Low pressure turbine (LPT) blade | [6,7,10–12] |
| | | | T700 compressor case | [7] |
| | | | Honeycomb panels (Reusable Launch Vehicles (RLV)) | [7] |
| | | Automotives | Casings in high pressure compressor | [9] |
| | | | Turbocharger wheel/turbine | [10,12–16] |
| | | | Turbine stator vane | [13] |
| | | | Exhaust valves | [14,16–19] |
| | | | Pistons | [9,14,17–19] |
| | | | Connecting rods | [9] |
| | | | Spring rings | [9] |
| | | Industrial gas turbines | Blades, Turbochargers | [1] |

**Table 2.** Comparison of TiAl alloys to superalloys [6].

| Property | TiAl-base alloys | Superalloys |
|---|---|---|
| Density (gm/cm$^3$) | 3.7–3.9 | 8.3 |
| Youngs modulus (GPa) | 160–176 | 206 |
| Yield strength (MPa) | 400–630 | 1000 |
| Tensile strength (MPa) | 450–700 | 1200 |
| Ductility (%) | 1–3 | 15 |
| Creep limit (°C) | 1000 | 1090 |
| Oxidation (°C) | 900–1000 | 1090 |
| Cost ($/lb) | 1300 | 20 |

join high-temperature materials include nickel and cobalt-based alloys. The LPM process begins with mechanical cleaning and selection of suitable filler material (gas atomized metal powder). Then, a slurry of the selected filler metal powder is applied to the cleaned surface of the geometry via syringe/spraying. This is followed by consolidation using the LPM process at high temperatures (typically 1100–1200 °C for 2–10 h) in a vacuum furnace. It was found that the LPM process produces bonding with the base material (vane edge) equivalent to alternative processes, and good mechanical properties due to fine-grained structure. However, it was possible to obtain the sound repair only after the post heat-treatment [25]. Shepeleva et al. [30] reported on plasma cladding to repair In713 shroud shelves surfaces of turbine blades. It was found that the plasma-treated surface finish was poor, and microcracks were present in the cladding surface. Nicolaus et al. [31] combined plasma spray and brazing, followed by aluminizing treatment methods to repair and improve the clad region corrosion properties. In this work, a plasma spraying process (APS) was used to coat NiCrSi (Ni650) onto the In718 substrate was followed by a brazing operation and application of an aluminizing coating. Afterwards, the brazed and aluminized turbine blade was subjected to a heat-treatment process that resulted in a nickel-rich deposition with low-cobalt aluminium phases. It was concluded that the coating and heat-treat methods enhanced the hot gas corrosion resistance of the repaired turbine blade. The entire process is time consuming and expensive [31]. Nicolaus et al. in a more recent study used a hybrid technology to repair turbine blades. In this case, the turbine blades were subjected to a two-stage hybrid technology for coating and improving the life. In the first step, a thermal spray coating is applied, followed by

machining. Then the blade is subjected to brazing and aluminizing to improve the blade's wear, heat resistance, and quality. It was found that voids were avoided by lowering the brazing temperature while coating [32].

Along with the aforementioned repair strategies, laser cladding is often used for repair, and to improve the surface characteristics of the metal components to reduce subsequent wear, corrosion, and erosion [29,30,33]. Numerous laser cladding investigations have been reported for reclamation of turbine blades using Co, Ni, Cu, Ti, and steel materials [26,30,34–36]. Nowotny et al. used the laser beam cladding process to repair the surface cracks, wear and damage of the titanium alloy (Ti6242) aero-engine parts. The heat-affected zone of the process is smaller than the TIG welding process. The results indicated that a laser cladding process could be developed that ensures good bonding between substrate and coating and crack-free surface [26]. Gorunov proposed the development of a wear-resistant coating for compressor blade. The laser cladding of the blade was performed under both continuous wave and pulsed laser operation using titanium powder. It was found that the coated aerofoil blade's high heat resistance and improved wear properties were due to the introduction of titanium aluminide and titanium borides. Also, with the addition of 2 wt.% addition of $Al_2O_3$ (particle size of 1–2 μm) to commercially pure Ti it was possible to produce a blade aerofoil coating with hardness 1.6 times greater than that of the substrate [34]. Shepeleva et al. [30] introduced wear-resistant coatings of damaged In713 turbine blades using laser cladding technique using a TRUMPF-2500 with a CW-$CO_2$ laser. The cladding of the turbine blades used laser energy density between $2.8 \times 10^4$ and $3.6 \times 10^4$ W/cm$^2$ and travel speed of 5–7 mm/s. The powder flow rate was maintained between 0.015 and 0.02 g/s. It was observed that the clad portion of the repair exhibited a uniform, pore-free microstructure with adequate bonding between the substrate and cladding region. Xiong et al. [35] reported laser cladding for the GH4133 based turbine blade repair using a ROFIN TR050 5 kW $CO_2$ laser. Various process conditions were considered, including laser power (1000–3000 W), travel speed (300–480 mm/min), and varying powder thickness, and the interfacial bonding of the clad to substrate was characterized. It was found the clad width, height and depth of melting increased with increase of laser power whereas clad width and depth of melting decreased with increase in travel speed. Further, a homogenous microstructure was obtained by subjecting the repair to an ageing treatment. Shishkovsky et al. [36] have reported depositing a TiN coating on a titanium substrate via laser cladding. They have witnessed that applying a graded coating with a Ti-$Al_2O_3$ mixture can improve hardness up to 20 HRC.

Even though the laser cladding techniques have proven themselves as a promising technology for the repair of various materials. However, there are issues with laser cladding such as: excess deposition of material in the clad region requiring post-deposition machining, time-consuming and expensive processing; and challenges in customizing the process for complex geometries. Table 3 presents the comparison of cladding processes, post-processing, advantages and limitations [21,37–39]. However, there remains a need to develop a cost-effective repair of the parts with good functional properties for TiAl based alloys.

Recently, researchers and engineers have been attracted to Additive Manufacturing (AM) technology due to minimal material wastage, design freedom, ability to produce near-net-shape components, complex parts, as well as ability to be used for surface modification, repair and refurbishment purposes [40–42]. Metal additive manufacturing can be classified into Powder Bed Fusion (PBF) and Directed Energy Deposition processes (DED) [43–45]. The PBF techniques cannot be used effectively for repair purposes [20,46]. However, DED techniques can be used for repair and remanufacturing, cladding/coating, surface modification etc. [47]. DED processing can produce a smaller heat-affected zone than conventional methods (e.g. arc welding), can be used to build a complex profile, and can produce high-quality cladding with superior properties [47,48]. Repairing complex shapes, including small grooves, slots, and aerofoil edges, is easily done in DED [20,47–50].

Researchers have shown that TiAl alloys are suitable for the aero-engine parts and can offer superior properties. This work reports the DED process for fabrication and case studies on the potential mending of TiAl alloys based on aero-engine parts.

## 2 Directed energy deposition additive manufacturing

Figure 1 shows the schematic illustration of the DED process in which a laser beam creates a melt pool on the substrate. The powder particles are coaxially fed through nozzles onto a melt pool. As the laser moves to the next location, the irradiated location gets solidified. The characteristics of DED are presented in Figure 2. DED offers several repair advantages over existing methods (powder metallurgy, Welding, HVOF, Plasma, etc.), as shown in Figure 3. Various researchers have shown that DED is a promising technology to restore the titanium aluminide damaged parts, such as turbine blades, propellers, and fuel injectors [22,37,58].

## 3 Directed energy deposition for fabrication of titanium aluminide components

Because TiAl intermetallic is inherently brittle in nature and difficult to fabricate conventional methods. PBF and DED are under considerations for the fabrication of TiAl components [57,60,61]. With PBF TiAl based low pressure turbine blade and fuel injector of aeroengine successfully fabrication is reported [10,60,62]. The DED technique has been evaluated for its ability to fabricate TiAl alloys aero-engine components [5,63–65]. TiAl's brittleness and high melting point make it challenging to fabricate and achieve the desired properties using any conventional routes [6,66,67], but DED has shown itself to be a promising method for fabricating TiAl based aero-engine parts [7,8,68–70]. Srivastav et al. [66] showed the DED capability of processing TiAl alloy for aero-engine applications.

**Table 3.** Comparison of various processes, their basic steps, advantages and limitations.

| Process type | Pre-processing | Post-processing | Advantages | Limitations | References |
|---|---|---|---|---|---|
| Electro spark process | Cleaning the workpiece for consistency of the part | A variety of post-processes need to be carried out to ensure dimensional stability | Prevention of liquid metal erosion and burr formation<br>Improved bonding | No automated applications<br>Liquid metal resistant electrodes required | [21,51] |
| TGAW, PAW, Brazing, Cladding | Cleaning the part from dirt, grease, etc.<br>Preheating the part to alleviate shrinking, cracking, distortion | Post heat treatment for stress relaxation<br>Grinding and polishing | Complex shapes parts repaired<br>Quality parts | Imperfections in the cooling<br>Heat affected zone<br>Blemish of the repaired part<br>Residual stress | [52] |
| Metalock process | Cleaning the part from dirt, grease, etc. | Repaired area peened flush and finish | No deformation and stresses<br>Suitable for cast iron<br>Can be used on-site | Cracked pieces are locked together and not fused to a single material | [21] |
| Robotic laser welding | Same as laser cladding | Non-destructive examination to check the integrity of weld | Dimensionally stable and high accuracy<br>Portable | Expensive<br>Limited to Nuclear system, Generator repair etc. | [53–55] |
| Laser cladding, Directed energy deposition (DED) | Cleaning of the material | Machining of excess deposition<br>Shaping of the finished part<br>Finishing shape of the geometry | Large gaps can be combined<br>Flexible for geometric changes<br>High accuracy<br>High deposition rate<br>Multiple materials deposition<br>Argon purged chamber<br>Small heat-affected zone (HAZ) | Expensive<br>Integrated approach to get best results<br>Support structure requires for undercuts and overhangs<br>Skilled labour | [21,22,38,56,57] |

Microstructural study of the specimens reveals a very fine heterogenous microstructure. Post-heat-treatment produces a uniform microstructure. They observed that variations in process parameters such as laser power and travel speed influence the microstructure formation [66]. Liu and DuPont [71] have reported reinforced carbide particle (TiC) in the TiAl matrix composites (Ti-48Al-2Cr-2Nb) deposited using DED technique. Due to high thermal stresses involved in the process the solid-state cracking was observed. They have mitigated these cracks by preheating (450–500 °C) the base plate/substrate. Balla et al. [72] investigated the effect of process conditions (power, scan speed) on microstructure, tribological and corrosion properties of laser-deposited TiAl alloy. They found that narrow processing space gives defect-free parts with good mechanical properties. Li et al. [73] and Rangaswamy et al. [74] have reported residual stress formation mechanism in metal additive manufacturing.

As shown in Figure 4a laser/electron beam melts the small area of powder (laser spot size 0.5 mm) during the heating, melted region expands and the peak temperature exists with within the melt pool at the laser irradiation. However, within the melt pool compressive strain is induced as results of peak temperature and surrounding material restriction. As can see from Figure 4c compressive strain reaches the peak become constant even though temperature is increasing. Thus, heating stage creates the compressive stress within the melted region. However, during cooling stage (Fig. 4b) when the laser source is removed from the melted region starts cooling rapidly and shrinkage tend to produce. In this process the induced compressive strain is converted into the tensile strain (Fig. 4d). The shrinkage of the material is partially restricted by the plastic strain produced during heating and surrounding cooled material. Finally melted region will have the tensile residual stress which is balanced by the

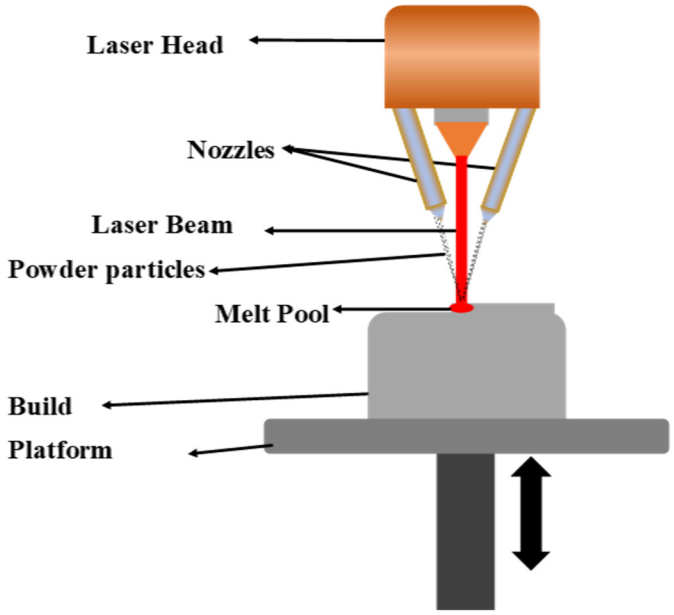


**Fig. 1.** Schematic illustration of DED technique.

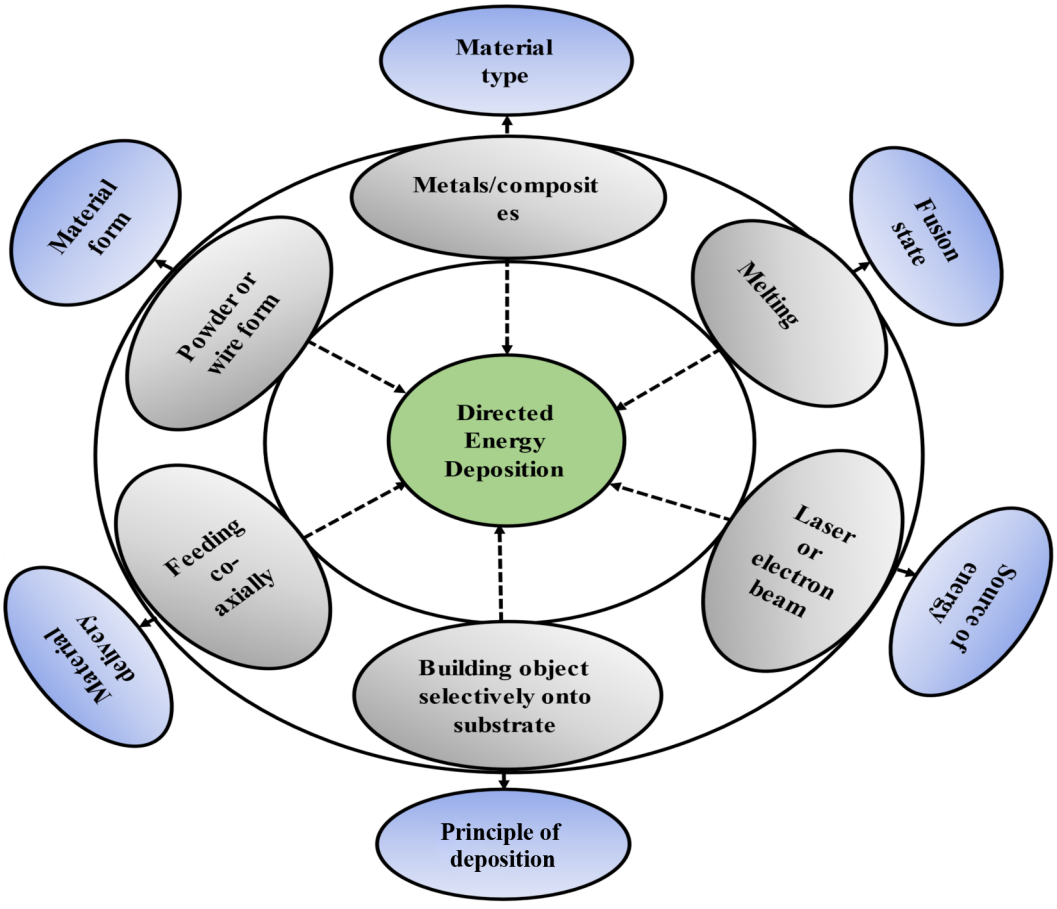


**Fig. 2.** Directed energy deposition features.

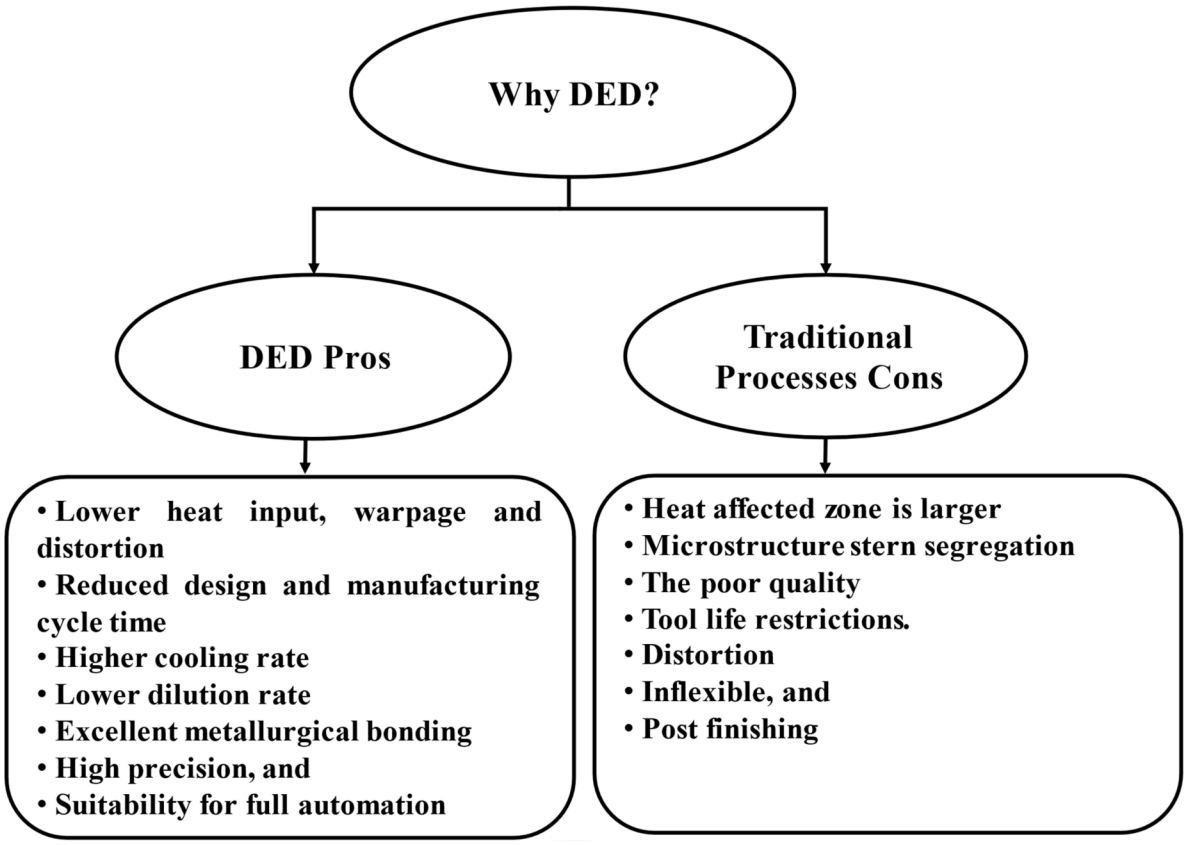


**Fig. 3.** Advantages of DED over traditional techniques [48,59].

compressive stress location. The induced tensile stress magnitude is depending on the temperature gradients and yield strength of the material. The deposition of bulk TiAl samples is challenge in DED as it involves the rapid heating and cooling rates generates the residual stress and distortion. Which is occurring due to variation in the thermal gradients between substrate and first layer or subsequent layers. Our earlier work on DED of TiAl is published on the successful overcome of thermal and solidification cracks of TiAl alloys thin walls [2,61,75]. Balla et al. have reported the TiAl deposition via DED process. It was used several process conditions to deposit the defect free TiAl parts. During the deposition have noticed the un-melting of powder, thermal cracks, over-heating and burning issues. The un-melting was observed when the energy density is below the $40\,J/mm^2$ and severe burning and overheating was noticed at $70\,J/mm^2$. Also, there were found the internal cracks of the deposited samples due to the high cooling rates generated the internal residual stresses and released as it exceeds the yield strength of the material. The energy density 40, 47, and $50\,J/mm^2$ have resulted in defect-free parts includes small amount of porosity and cracks. In one of our paper Balichakra et al. [57] reports the cracks in melt pool due to the high temperature gradients and cooling rates of laser surface melting of TiAl in DED. SEM images of the melt pool reveals the presence of the cracks in all process conditions. These cracks are originating from the top of the melted region (remelted region) due to the rapid cooling rates within the melt pool in the order $10^5\,K/s$. The cracks in the melt pool designated the internal stresses are released as it exceeds the yield strength (400 MPa) of the TiAl material. It was also noticed that the laser power increased from 200 W to 400 W. The length of the cracks was increased. Which shows that the cracks are susceptible to the laser power. In an another paper by the same author [61] have reported the crack-free surfaces and internal zone of the TiAl thin wall samples is reported. The fabrication of near net shape parts in DED required optimum process parameters [76]. The base plate or substrate preheating is preferred which reduces the thermal gradients and residual stresses in DED printed parts [77]. Post heat-treatment also a choice to mitigate the residual stresses in the samples. Thereby enhancing the fatigue life of the parts. Process parameters optimization is essential step in DED processing of TiAl alloys. Several researchers reported on the optimum process parameters for defect free samples. Table 4 presents the consolidated difficulty, reason and remedy for manufacturing of TiAl alloys.

In another study Qu et al. [85], fabricated intermetallic TiAl alloys for aerospace applications using the DED process. As-deposited and heat-treated specimens were characterized and have reported fully dense columnar grains with a fully lamellar structure. Thomas et al. investigated the effect of process conditions in DED of Ti-48Al-2Cr-2Nb alloy for aero-engine parts. Deposition involves the large thermal gradients and cooling rates that result in high residual stresses. The induced stresses exceed

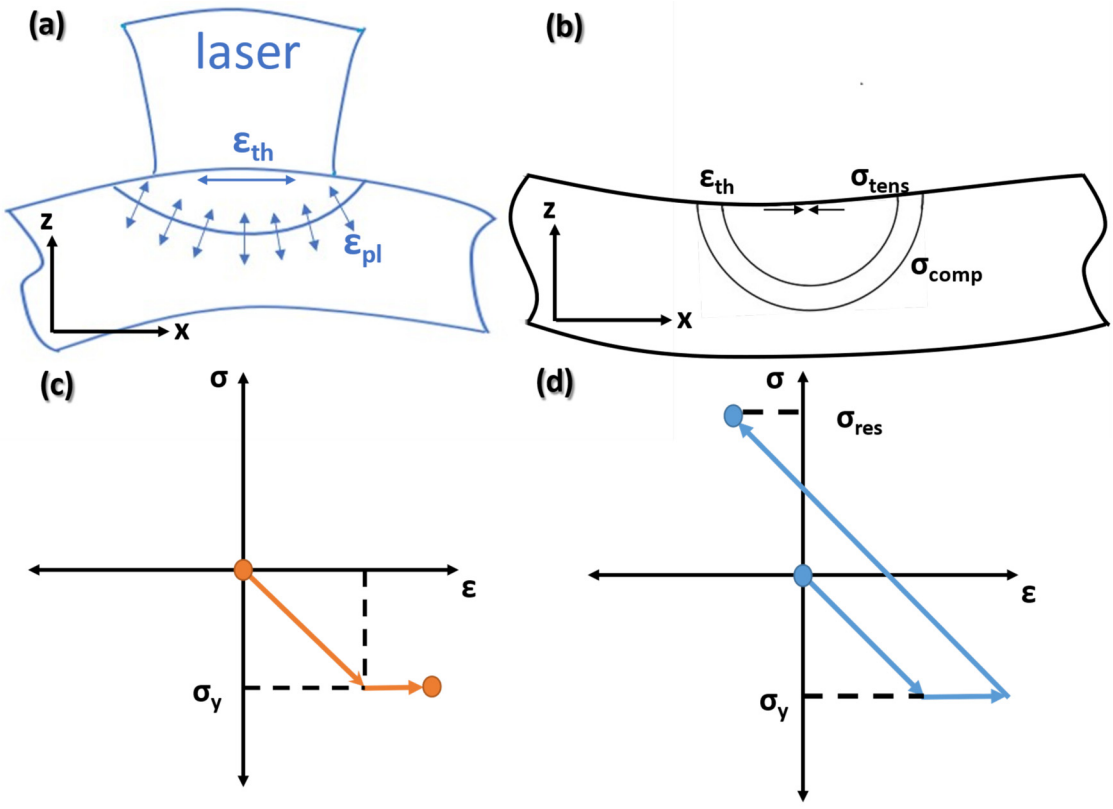


**Fig. 4.** Illustration of residual stress development during (a and c) Heating stage (b and d) Cooling stage [73,74].

the yield strength of the material, which leads to cracks in part. However, they demonstrated that they could control thermal gradients by adjusting the laser beam movement (exposure time) and fabricating defect-free parts. The rapid-cooling rates in the process result in fine grain structure and also yield higher hardness [86]. Abdulrahman et al. employed a DED technique to deposit TiAl powder on a CP titanium base plate with different process parameters [87]. It was found that the microstructure of the specimens majorly consists of γ with a small amount $\alpha_2$ phases due to the high cooling rates while deposition [87]. Tlotleng reported on the innovative way to produce titanium aluminide alloy from elemental powders (Ti and Al) via the DED process [88]. As-deposited TiAl cube samples were subjected to characterization before and after heat treatment. A non-uniform microstructure was noticed along the build direction. After heat-treatment, different grain sizes and phases were found in the sample's bottom, middle, and top. Tlotleng et al. [89] presented the microstructural and hardness properties of γ-TNB based turbine blades produced via the DED process. The microstructure of the turbine blades was found to be lamellar ß and γ, α and ß (multiphase). The hardness of the as-deposited turbine blade was between 526 HV2 and 435 HV2, which was higher than heat-treated ones. Liu et al. [90] used a DED technique to investigate Ti48Al2Cr2Nb alloy with the addition of Ta (up to 5%). It was found that Ta addition into the Ti4822 increased the tensile strength by 1.65, 2.08 and 1.9 times (677 MPa, 651 MPa, and 538 MPa), at room temperature, 750 °C and 850 °C respectively [90]. This was attributed to the changes in microstructure with the addition of Ta, which caused the lamellar thickness to increase, with an accompanying decreased in lamellar length. The $\alpha_2$ phase formed an ultra-fine continuous lamellar structure to a short lamellar and an equiaxed structure [90]. Chen et al. [91] has presented the fabrication of a γ-TiAl alloy based on Ti-47Al-2Cr-2V (at%) powder aero-engine blade and disk deposited on a Ti-22Al-25Nb (at%) alloy substrate using the DED process. The nano-hardness of the deposited disk and blade for layers 1, 2 and 3 was reported as $7.55 \pm 0.20$ GPa, $4.96 \pm 0.27$ GPa, and $4.85 \pm 0.08$ GPa, respectively. The variation of the hardness value from the substrate to layer 3 in the build direction is due to the various phases present (variation of cooling rates) in the disk and blade. The substrate has the O, B2 and $\alpha_2$ phases; layer 1 has ß/B2 matrix with $\alpha_2$ and γ phases, layer 2 has ß/B2, γ phases and $(\alpha_2 + \gamma)$ lamellae, and layer 3 has ß/B2, γ phases and $(\alpha_2 + \gamma)$ lamellae [91]. Huang et al. investigated the influence of adding $L_aB_6$ nanoparticles into the γ-TiAl alloy powder in the ratio of 99.5:0.5. The DED process was used for fabrication of samples. The 0.5 wt.% $L_aB_6$ inoculations improved compressive strength, ultimate strength and fracture strain by 29%, 12.4% and 61.9%, respectively. This is due to the microstructure refinement from coarse lamellar colonies into the refined equiaxed grains [92]. Another DED techniques called electron beam freeform fabrication ($EBF^3$). Xu et al. [93] have showed the in-situ fabrication of TiAl alloy via dual-wire electron beam freeform fabrication ($EBF^3$). The dual phase Ti-(37−52) at% Al

**Table 4.** Issues, reasons, and possible remedy for DED of TiAl alloys.

| Issues | Reasons | Remedy | References |
|---|---|---|---|
| Residual stresses | High thermal gradient and cooling rate, reheating, difference in substrate and layer thermal gradients | Substrate/base plate preheating<br>Additional energy source for melting | [73,78] |
| Crack initiation/ Solidification cracks | Residual stresses<br>Pores | Optimum process parameters<br>Post heat treatment processes. | [2,79–81] |
| Balling | Insufficient energy density to melt the TiAl powder | Process parameters optimization | [8,79,82] |
| Surface roughness | Stair casing effect<br>Improper process parameters | Optimized process parameters<br>Build orientation<br>Post machining and heat treatment | [61,83] |
| Porosity | Poor melting between layers<br>Inappropriate process parameters<br>Gas entrapment while atomization process<br>Oxygen pickup during the melting process | Process parameters optimization<br>HIP process after AM process<br>Gas purification system for atmosphere cleaning | [2,79,84] |

alloys were prepared by feeding Ti and Al wires into the melt pool created by electron beam under vacuum atmosphere. Microstructural analysis of Ti-49 at% Al and Ti-52 at% Al samples found that the lamellar structure major composed of γ and $\alpha_2$ phases, as shown in Figure 5a. The $\alpha_2$ phase is mainly formed due to the rapid solidification. Utyaganova et al. [94] have tried to in-situ alloying of AA5083 (aluminum alloy) and Ti-6Al-4V (Titanium alloy) to produce γ-TiAl using wire electron beam additive manufacturing (WEBAM). The prepared γ-TiAl samples subjected to the microstructural and hardness study. It was found that the inhomogeneity distribution of intermetallic phases γ-TiAl and $TiAl_3$. The top to the bottom i.e., along the build direction is showed wavy hardness profile due to heterogeneous composition formed as a result of complex thermal cycles and repeated heating of layers. Further, samples free from porosity and oxidation contamination as the deposition is taken place under the vacuum condition.

Wire Arc Additive Manufacturing (WAAM) was originally a welding technique. Recently many researchers have claimed the DED technique by depositing the parts with multiple layers and multiple tracks [9–14]. Wang et al. [14] presented the binary TiAl alloy fabrication via the twin-wire plasma arc additive manufacturing (TW-PAAM) process. The XRD results indicate the presence of $\alpha_2$ and γ phases. Ti-45Al sample reveals the inhomogeneous microstructure with an equiaxed grain and dendritic grains consisting of $\alpha_2$ and γ phases. It was observed the presence of the intergranular cracks due to higher residual stresses generated from rapid cooling rates, as shown in Figure 5b. Wang et al. [15] showed the production of functionally graded titanium aluminide via WAAM based gas tungsten arc welding (GTAW) technique. The 1 mm and 0.9 mm diameters of Ti and Al wire were fed directly to the weld pool while depositing the samples. The argon shielding was used to avoid the contamination of the samples. The angle between the two wire feeding nozzles (Ti and Al) were maintained 60° to have the stable melt pool. The 25 mm × 130 mm × 10 mm size of various samples were fabricated by varying the Al concentration at constant current of 120 A and traveling speed of 100 mm/min. Metallographic study of Ti-47 at% Al alloy sample reveals the lamellar structure consisting of γ and $\alpha_2$ phases Wang et al. [14] presented the binary TiAl alloy fabrication via the twin-wire plasma arc additive manufacturing (TW-PAAM) process. The XRD results indicate the presence of $\alpha_2$ and γ phases. Ti-45Al sample reveals the inhomogeneous microstructure with an equiaxed and dendritic grains consisting of $\alpha_2$ and γ phases. The intergranular cracks were observed due to higher residual stresses generated from rapid cooling rates (as shown in Fig. 5c). With sporadic γ interdendritic phases surrounded. Interestingly, it was not found any microcracks in the samples. Henckell et al. [12] investigated in-situ production of titanium aluminide using gas metal arc welding additive manufacturing. Titanium (99.6 pure) and Aluminium (99.5 pure) 1 mm diameter wires were fed simultaneously to the surface of the Ti grade 2 base plate for the fabrication of TiAl. It was observed that the cold crack in the samples was due to hot wire feeding. The microstructure of samples purely depends on the Al percentage. It was found that the dendritic structure consists of γ and α phases, as shown in Figure 5d. After heat-treatment, it transformed to the $\alpha_2 + \gamma$ phase. It was concluded that the titanium aluminide was produced successfully using GMAW-AM; further investigation is required to reduce the cold cracks. Cai et al. [11] have reported on the in-situ synthesis of

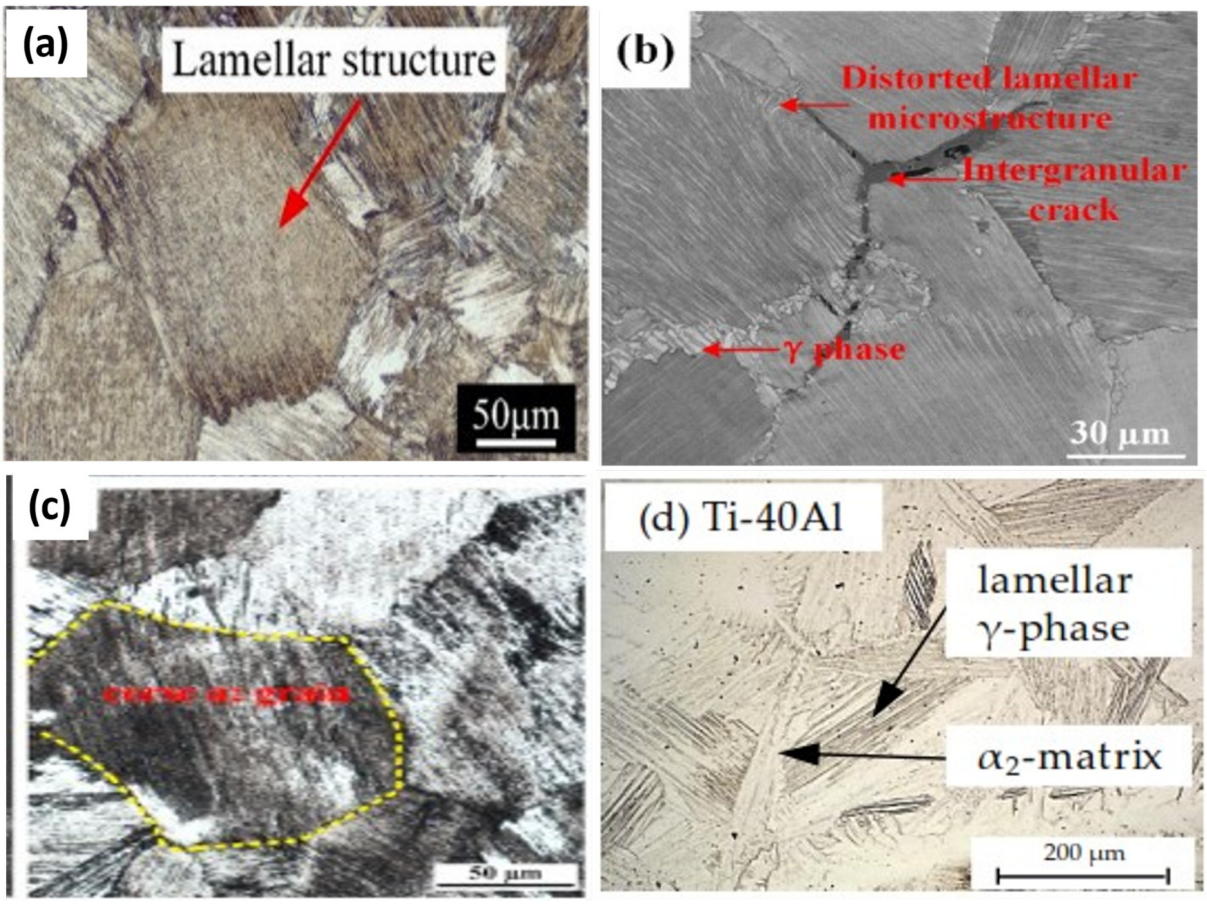


**Fig. 5.** Typical microstructure of TiAl alloys processed in (a) EBF$^3$ (Xu et al.) (b) Twin wire plasma additive manufacturing (Wang et al.) (c) Gas tungsten arc welding (GTAW) (Wang et al.) (d) GMAW (Henckell et al.).

**Table 5.** TiAl state-of-the-art alloys [6].

| TiAl Alloys | Properties enhanced |
|---|---|
| Ti48Al2Cr2Nb (48-2-2) | Fracture toughness, ductility and oxidation resistance |
| Ti45Al(5–10)Nb (γ–MET) | High creep, fatigue, temperature strengths and good oxidation resistance |
| Ti(45–47)Al10Nb (TNB Alloy) | High creep, temperature strengths, and oxidation resistance |
| Ti45Al2Mn2Nb0.8B (XD$^{TM}$ TiAl) | Ductility, high temperature strength, stiffness, creep, and oxidation resistance |

TiAl-based alloys using Wire Arc Additive Manufacturing (WAAM). TIG welding current 120 A, voltage 9–10 V, the travel speed was 100 mm/min, and the pre-heating of the base plate temperature was maintained at 450 °C. It was fed the two wires (Ti64 and Al) of 1.2 mm diameter in-situ coaxially to the surface of the base plate from either side of the power source. The microstructure analysis of the as-deposited samples reveals the $\alpha_2/\gamma$ lamellae. The feeding Al wire is critical due to the influence of the distribution of the $\gamma$ and $\alpha_2$ phases. Wang et al. [16] have proposed the titanium aluminide in-situ alloy preparation by adding a ternary element (Al). They have used the WAAM technique to fabricate the Ti45Al2.2 V alloy sample. For this used Ti6Al4V alloy with Al wires of 1.2 mm and 0.9 mm diameters, respectively. Al feeding composition was controlled with the feeding speed of wire. The constant voltage and current of 120 A and 13 V were used, respectively. It was successfully fabricated the titanium aluminide (Ti45Al2.2V) crack-free samples in WAAM. The metallography investigation reveals the fully lamellar structure with the interdenticle $\gamma$ phase. Further, heat-treating increases lamellar spacing from about 75 nm to 220 nm. Numerous researchers have reported on processing of various TiAl alloys, and results are summarized in Table 5 [6].

Second, third and fourth-generation alloys have been investigated due to their exceptional properties, such as low density, high elastic modulus, good oxidation and corrosion resistance, and high service temperature. Hence, GE's reported the fabrication of a TiAl-based turbine blade and fuel injector for their GENx Jet engine [62,95].

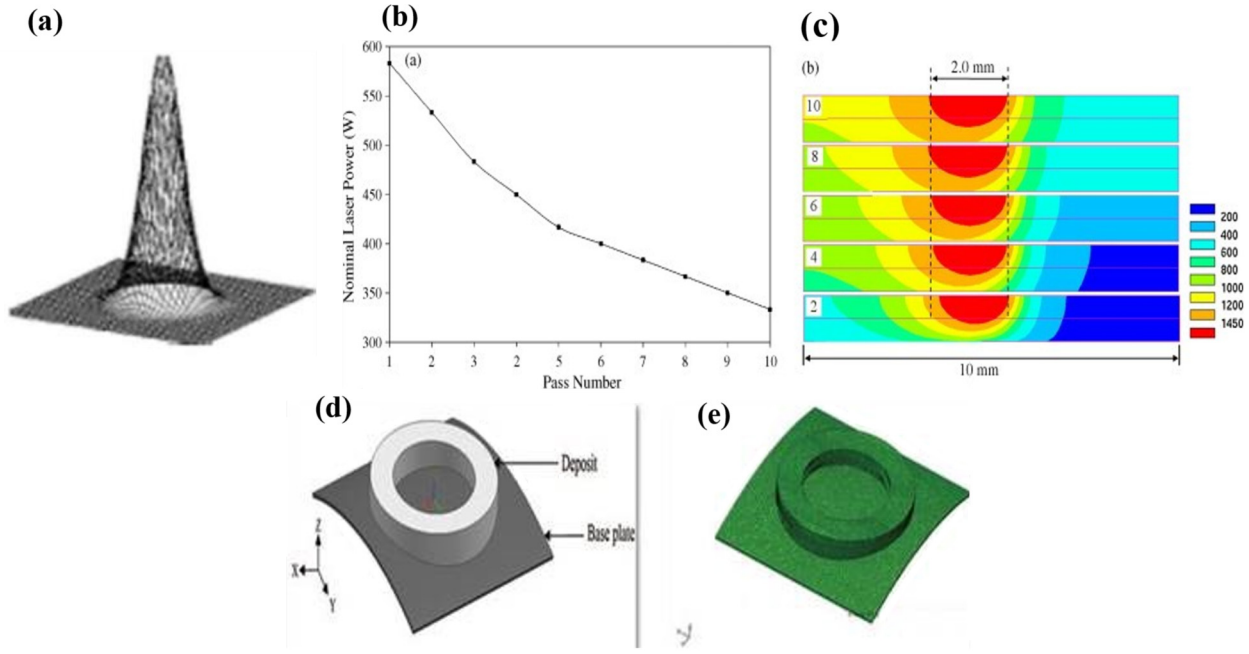


**Fig. 6.** (a) Gaussian distribution beam mode profile for moving laser source [109]. (b) Minimum laser power required to maintain the steady melt pool at each pass. (c) Melt pool size and shape at the centre of each layer (2, 4, 6, 8, 10) [110]. (d) IN718 deposited aero component and (e) FE model [111].

The literature on the DED of TiAl alloys has been reported. TiAl is an inherently brittle material that leads to cracks, delamination, and residual stress formation during deposition. Extensive experimentation is required to obtain the desired process parameters, which leads to material waste, time consumption, and cost. Further to address these issues, researchers have reported numerical modeling of DED processes for deposition of TiAl alloys. The optimum process parameters (laser power, scan speed, hatch spacing, powder flow rate, layer height, etc.) are obtained to produce defect-free TiAl parts. The following section reports the numerical modeling of the DED process is reported.

## 4 Thermomechanical modelling of DED process

Several researchers have reported the 3D transient thermo-mechanical analysis of Directed Energy Deposition (DED) of various materials (Titanium alloys, Inconel, Stainless Steel, Waspaloy, Tool steel, etc.) to predict the thermal history, melt pool, cooling rates, residual stress and distortion [96–108]. Roberts et al. [109] hey have assumed a laser beam as a Gaussian profile in their modeling work (Fig. 6a), which is a bell shape. The laser beam intensity is maximum at the center and exponentially reduces heat intensity radially away from the laser beam center.

Wang et al. [110] have carried out a 3D-transient thermal analysis to optimize the DED process for obtaining the steady melt pool dimensions. The moving laser heat source was modeled as a Gaussian distribution with a conical shape. It used the element birth and death technique to simulate the DED of an SS410 alloy plate. Melt pool predictions demonstrate that the steady melt pool results in uniform microstructure and thermal distortions. Further developed FE model showed that maneuvering of laser power during each pass maintains the constant melt pool dimensions (Fig. 6b). Mukherjee et al. [104] have reported on the reduction of thermal distortion during additive manufacturing of parts. They have considered two major parameters, including laser and travel speed, to understand the effect on Marangoni, temperature, and thermal strain in non-dimensionalized form. It was found that the as the laser power and travel speed increase results in a reduction of Marangoni number and non-dimensional temperature and a decrease in thermal strain. Mukherjee et al. [112] carried out a 3-D transient thermo-fluid-structural analysis of Ti6Al4V in the DED process. It was found that predicting the thermal history helps control residual stress formation. Ahmad et al. [113] have presented numerical modeling of wire-fed additive manufacturing of Titanium alloy to predict residual stress and to validate with measured residual stress. It was found that compressive stresses in the core and tensile stresses in the interface (deposit and substrate). Kamara et al. [107] have reported the Thermo-elasto-plastic analysis to estimate the DED process of Waspaloy parts. The FE model could predict residual stress characteristics with an average error of 20% with the measured ones. Marimuthu et al. [111] investigated the influence of process parameters using finite element analysis on distortion and residual stresses in DED of IN718 aerospace parts. FEA of various scan strategy was achieved a uniform thermal history and low distortion. The

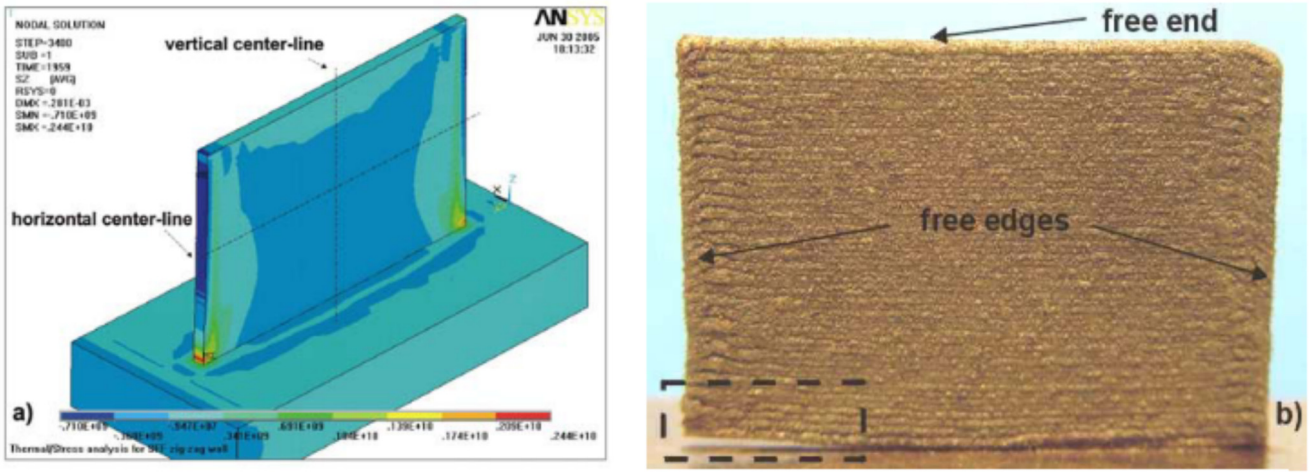


**Fig. 7.** (a) Build direction residual stress contour (b) Delamination of thin wall sample from the substrate [115].

effect of process parameters on distortion resulting from residual stress in 3-D IN718 aero components, as shown in Figures 6d and 6e.

Lu et al. [114] have presented a three-dimensional thermo-mechanical analysis of the DED process. They have simulated thin walls deposition on different substrate structures to understand the residual stress and distortion characteristics. The substrate structure was found to reduce and increase the stresses due to heat accumulation during deposition. Reducing the substrate's size was recommended to lower the residual stress formation. Also, hollow substrate structures slow the heat flow from the substrate to the table. Thereby substrate will be heated up, reducing the thermal gradients difference between the walls and substrate.

Zekovic et al. [115] used accurately sequentially coupled thermo-mechanical analysis of the DED process of the H13 tool steel. The FE model included the boundary conditions such as conduction, convection, non-linear material properties, and element birth and death technique to predict the temperature, distortion, and residual stresses. Figure 7a shows the maximum temperature at the thin wall sample interface. Predicted residual stresses exceed the yield strength of the material at the interface of the thin wall. Thus, the delamination that occurred in the sample is shown in Figure 7a. Predicted residual stresses exceeds the yield strength of the material at the interface of the thin wall. Thus, delamination occurred in the sample is shown in Figure 7b. Jing et al. [116] used a sequentially coupled thermomechanical model to predict and understand the behavior of substrate structure for the deposition of TiAl6V4 in the DED process. It was concluded that the long strip with holes substrate structure reduces the tensile residual stress by 20%. Also, one end of the substrate is fixed, and the other end is made free, which decreases the further residual stresses.

Sakin et al. [117] Finite Element Modeling of WEBAM process carried out to predict the temperature, cooling rates, and grain morphology of the Ti6Al4V alloy. Thermal history prediction compared with the thermocouple measurement showed an average error of 3.7%. Predicted residual stresses and distortion were in good agreement with the experimental ones with a deviation of 100 MPa and 0.05 mm, respectively. Figures 8a and 8b shows the predicted and measured contours. It was concluded that the developed finite element model is helpful in process parameters optimization for manufacturing and repair applications. However, a few papers reported on numerical modeling of DED of titanium aluminide intermetallic alloy [2,61,118]. Mallikarjuna et al. [2] have shown the thermomechanical modeling of the DED of TiAl alloys. The various process parameters were considered to understand the effects on temperature and residual stresses. The estimated residual stresses were increased with laser power (200–300 W) and decreased with an increase in the velocity (8–12 mm/s). The predicted residual stress contours are shown in Figures 8c–8e. They have predicted the melt pool, temperature, and residual stresses and validated them against the experimentally measured residual stresses. Yan et al. [81] conducted a thermal analysis of the DED of Ti48Al2Cr2Nb alloy to predict temperature and cooling rates. They have used the element birth, and death technique and a laser heat source assumed as a Gaussian distribution for the thermal analysis. The predicted cooling rates have shown the decent agreement with of measured cooling rates. Thus, possible to fabricate the crack-free TiAl parts. Wang et al. [119] have reported on numerical modeling and experimental study of LSM of Ti-47Al-2Cr-2V alloy. The microstructure of dendritic arm spacing has been predicted with various process parameters. The temperature gradient plays a significant role in the formation of dendrite arm spacing. Recently many researchers proposed numerical modeling of the DED process to predict process variables that influence the melt pool, cooling rates, temperature cycles, residual stress, and distortion of various materials, which have been reported elsewhere [120,121].

From the thermomechanical modeling of the DED process can be concluded that the literature showed several computational methods and examples of finite element modeling for directed energy deposition of various materials to optimize the process conditions for the testimony of the crack-free samples. Thereby mitigating

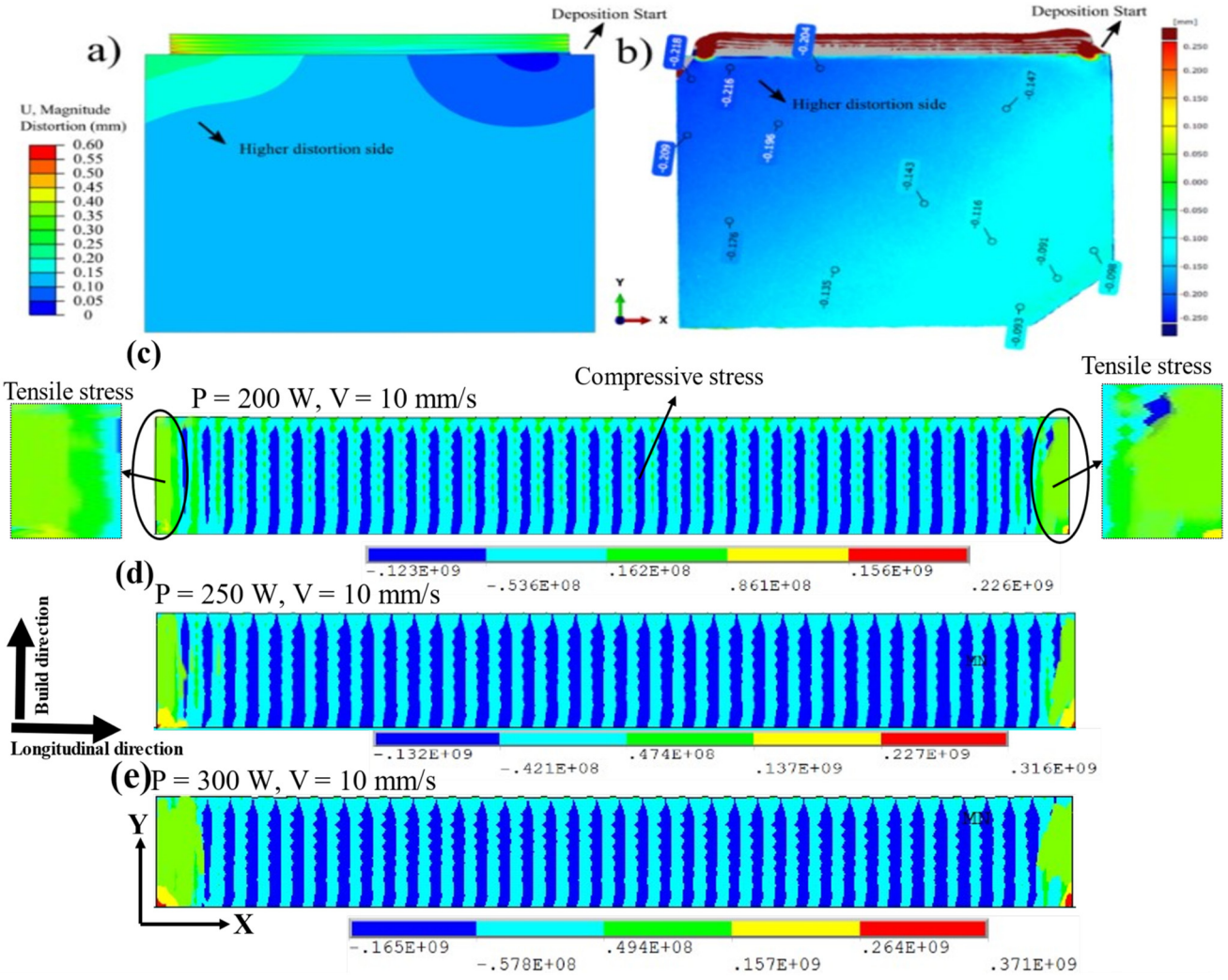


**Fig. 8.** (a) Prediction of distortion. (b) Measured distortion map [117]. (c–e) Contours showing the infleunce of laser power in logitudinal and build direction on residual stress [2].

the extensive experiments, time, and cost involved in a component's manufacturing/remanufacturing. Further, within the author's knowledge, few papers exist on numerical modeling of the DED process for the fabrication of TiAl alloys. The following section discuss the why reclamation is paramount via DED.

## 5 Why reclamation of aerospace components using directed energy deposition

The TiAl based aerospace and automotive components (as presented in Tab. 1) includes blades, fuel injector, blisk, turbocharger, exhaust valve, connecting rods are expensive [6,7]. During functioning these components subjected to oxidation, corrosion, creep, impacts, erosion, high temperature and stresses would cause wear, fatigue, cracking or defects during their service [5,58]. Thus, these high performance and expensive components to be scrapped. The high costly materials, complex processing routes and labour intensive involved in production of components. Hence reclamation of these components is necessary rather than the replacement [20]. Conventionally various welding techniques such as tungsten inert gas welding, plasma arc welding, oxy fuel thermal spraying, electron beam welding used for the restoring the high value components. These techniques have limitations like cracks, residual stresses, large heat affected zone, large puddles, spattering and non-uniform spreading [51,52]. Importantly TiAl inherently brittle difficult process using conventional techniques. The researchers trying to find alternative routes for processing of TiAl alloys [10,17]. Directed energy deposition (DED) is being used for the deposition of TiAl complex geometries and same machine utilized for the repair as well [37,122]. Hence, DED provides opportunity to restore the worn out/defect parts layer-by-layer with controlled material deposition, low distortion, and low heat affected zone [20,123]. The component itself is acts as base plate and material is added in the worn out/defect area locally.

Rauch et al. [123] have investigated the repair of aeronautical components via DED. The flow diagram of the reclamation procedure is proposed is shown in Figure 9.

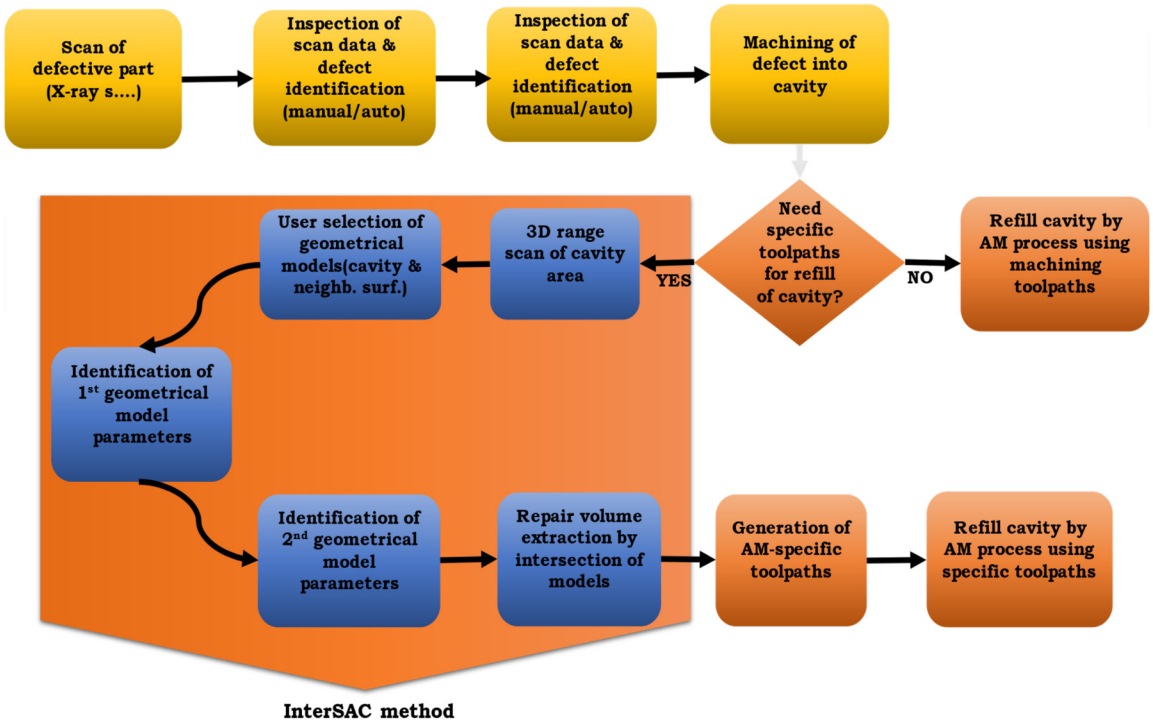


**Fig. 9.** Proposed semi-automatic reclamation strategy in DED [123].

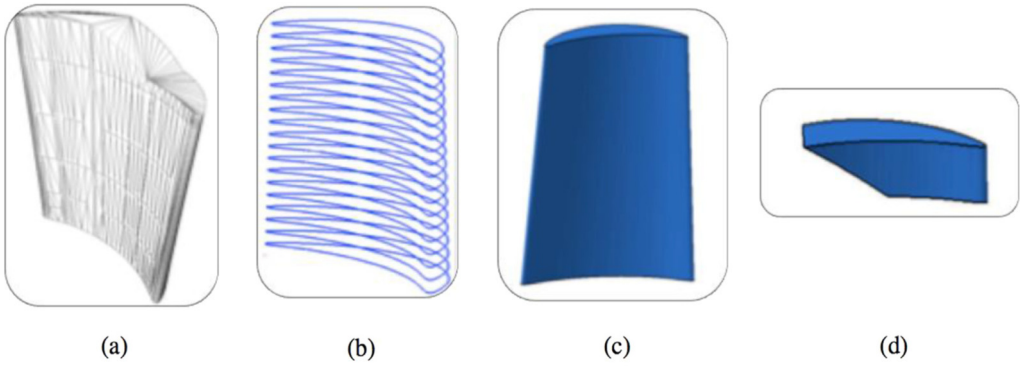


**Fig. 10.** Procedure for creating a parameterized geometric model required for defect repair: (a) Acquire point clouds and generate mesh, (b) Extract PCS from non-defective region and extrapolate missing section, (c) Reconstruct repaired model, and (d) Extract Boolean difference between (a) and (c) To obtain the repair volume [124].

The major issues with the restoration of the components are the different requirements unlike the usual fabrication method. This is the initial problem for the smooth functioning of the repair. The following flow chart reported for the mending of Ti6Al4V parts via DED [123]. The semi-automated repair technique to identify the defective, scan the area, machining the readiness for the repair, create the local cavity, generate the scan path for deposition [123].

In another work was demonstrated the aero-foil damaged turbine blade repaired via DED, is shown in Figures 10a–10d. Initially scanning of defective blade for the geometry reconstruction. The generated point cloud data transformed into a triangular facets representation provide the shape of the blade. Then extrapolate the missing section of the blade using PCS algorithm. Followed by the construction of blade in CATIA software. Finally, subtraction (Boolean) of damaged blade region by comparing Figures 10a and 10c. Thereafter repair of the blade using DED process locally. Figure 11a–11c shows the original turbine blade, damaged blade tip and repaired blade via DED [124]. Therefore, DED could be a potential technique to restore high-value components at a low cost and rapidly. The DED machine can be used for deposition, cladding, surface modification and repair applications However, further investigation is required to obtain the standard operating procedure. The following section presents the importance of the laser surface melting or cladding of TiAl alloys.

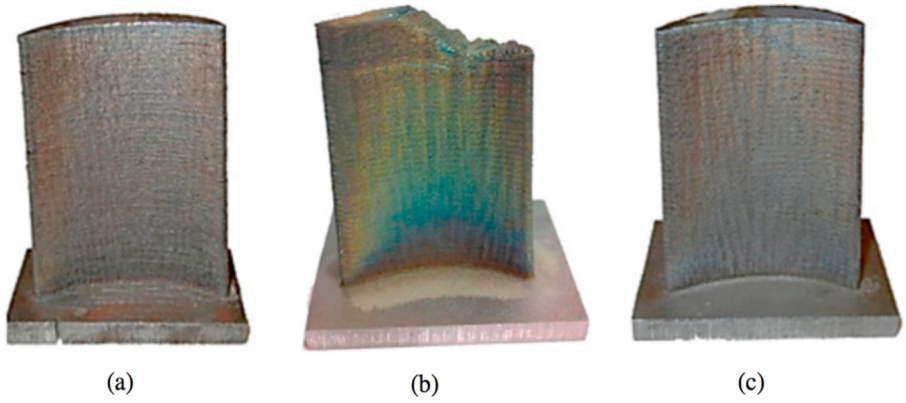


**Fig. 11.** Turbine blades fabricated with DED (a) Original blade, (b) Damaged blade tip and (c) PCS repaired blade [124].

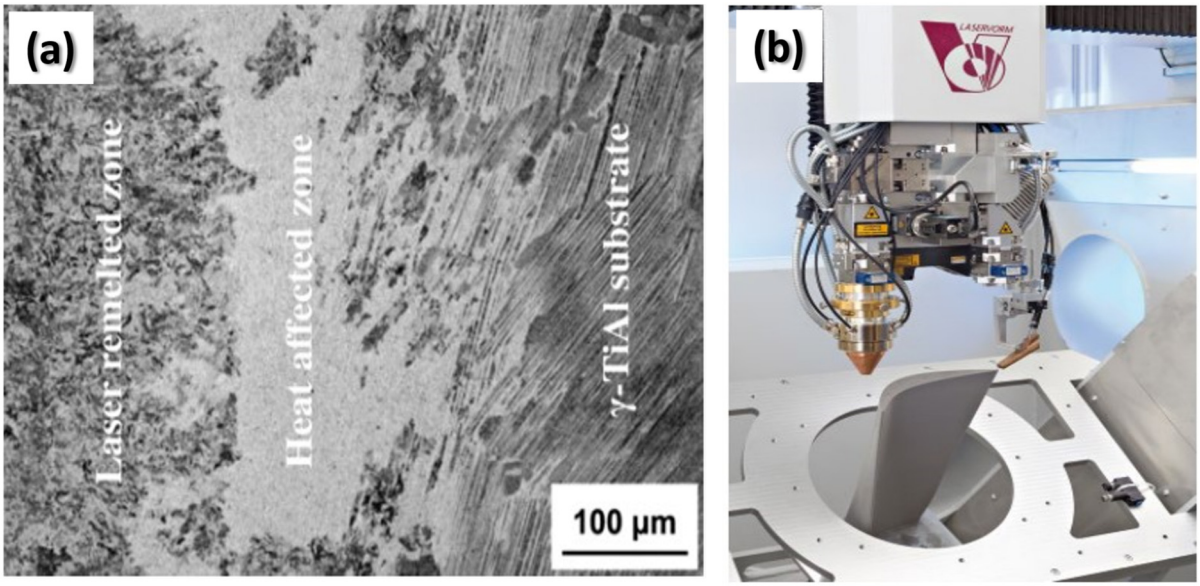


**Fig. 12.** (a) Cross sectional view of the SEM image of the laser surface melted TiAl [127] (b) Shows the repair of turbine blade by DED approach (Reproduced with the permission of Author) [122].

## 6 Laser surface melting/cladding of titanium aluminide

Carcel et al. [125] investigated the cladding of titanium aluminide (Ti-48Al-2Cr-2Nb at.%) powder on Ti-6Al-4V alloy base plate to obtain desired wear property and high temperature application. While cladding witnessed the crack formation due to the high cooling rates of the order $10^5$ K/s. Optimum process conditions for the cladding of TiAl powder on base plate were arrived via correlating the scan speed and cooling rate. The cladded region showed a fine dendritic microstructure with an arm spacing of <0.5 μm. The microhardness of the clad is 450 HV achieved compared to the base plate (340 HV). It was also observed that preheating of base plate (Ti-6Al-4V) abridged the formation of crack in the clad region. Li et al. [126] have reported that the laser surface modification of Ti–46.5Al–2Cr–1.5Nb–1V surface for the diffusion bonding with the nickel-based alloy. The laser surface modified region consists of fine dendritic $\alpha_2$-$Ti_3Al$ and γ-TiAl phases. It was found that at 1173 K with a pressure of 60 MPa in 1 h improves shear strengths of the bonds, and sound bond laser surface modification. Luo et al. [127] have studied the laser surface melted TiAl sample for the diffusion bonding with the nickel base casted alloy (Ni56Cr7Ti15Al22). Laser melted TiAl surface region have showed the dendritic and cellular structure with major constituents of $\alpha_2$-$Ti_3Al$ (Fig. 12a). Post annealing process modifies the existing the $\alpha_2$ phase into the fine γ-TiAl phase. The transformed fine γ-TiAl grains offers the good structural bonding with the base via diffusion bonding. Also high shear strength between the coating and clad region due to the laser surface melting [127]. Mallikarjuna et al. [57,128] have reported that the a plate $20 \times 20 \times 5$ mm$^3$ specimen were fabricated using electron beam melting process. Then the same specimen was used for the laser surface melting using LENS

**Table 6.** Process parameters used in DED and PBF to build TNM-B1 alloy components [22].

| Process | Laser spot diameter (mm) | Power (W) | Travel/Scan speed ($mms^{-s}$) | Layer height (mm) |
|---|---|---|---|---|
| DED | 0.6 | 66 | 8.33 | 0.25 |
| PBF | 0.09 | 200 | 1200 | 0.03 |

technique (DED process) at various laser powers (200, 300, 400 W) at constant velocity. The melt pool, temperature and cooling rates were extracted. Thermomechanical analysis was carried out using ANSYS software. Predicted melt pool size increased with laser powder 200 to 400 W due to the high energy density. Comparing the numerical modeling and experimental results have calculated the coefficient of thermal expansion of TiAl i.e., about 0.13. It was also reported the cracks within the melt pool is due to the stress exceeds the yield strength of the material thereby cracks within the remelted region. Within the authors knowledge it was found that the limited literature on laser surface melting of TiAl alloys.

## 7 Case studies on directed energy deposition to repair intermetallic γ-titanium aluminide aero-engine components

Several researchers have reported on the directed energy deposition (DED) of TiAl alloys [5,66,72,76,129,130]. There is a limited data exists on reclamation of TiAl alloys via DED [122,131–133]. Hence, the following few papers has been identified and discussed as case studies. Rittinghaus et al. [132] presented the possibility of titanium aluminide-based jet engine blade reclamation. They used a DED process to fabricate TiAl samples and evaluated the effectiveness of laser-based DED repair. Samples exhibited fine microstructures with two phases, primarily γ-TiAl grains and $\alpha_2$-$Ti_3Al$. It was observed that a different grain size within the sample was produced as a result of the layerwise deposition. Based on the flexibility in the process, they have concluded that laser-based DED is a technology that has potential to be used for reclamation of TiAl engine blades.

Kimme et al. [122] have investigated laser surface cladding technology to repair titanium aluminide turbine blades, as shown in Figure 12b [122]. They used three materials for the repair: TiAl (48-2-2), Ti-4522XD and TNM-V3B alloys. The laser cladding system was equipped with inert gas flow, automated scanning technology, and they found that preheating and temperature control for the blade repair resulted in high quality and superior properties in the repaired region. The inert gas supply via nozzles was insufficient to properly shield the deposition from oxidation effects on the preheated part. This was addressed using a modularly constructed inert gas tub, which provided argon gas flow from all sides. The oxygen in the gas tub was monitored, thereby ensuring a high quality of inert gas. The blade and substrate were preheated using a combination of radiant heating, inductive heating, laser local heating to raise the temperature of the substrate to 500–900 °C to avoid thermal-gradient induced cracking. The five-axis laser system was equipped with a modular laser power control to control local temperature cycles. Careful control of thermal gradients was necessary to produce defect-free repairs. Overall, they have cost-effectively repaired damaged blades with base component properties [122]. Rittinghaus et al. [22] have reported using hybrid manufacturing technology (i.e. a combinations of powder bed fusion (PBF) and directed energy deposition (DED)) for TiAl turbocharger wheel manufacture and repair. A TNM-B1 alloy (Ti-43.5Al-4Nb-1Mo-0.1B (at.%)) was chosen as the target component. The powder particles size was between 20–90 μm in DED and 20–80 μm in LPBF processes. The DED sample is built on the TNM substrate, whereas the PBF sample is built on Ti6Al4V alloy substrate. Table 6 presents the process parameters used to build the component in DED and PBF.

In both cases, preheating to 900 °C was performed prior to AM processing. The comparison of the DED and PBF microstructures is shown in Figures 13a and 13b. Microstructural analysis of the samples reveal lamellar grains includes $\alpha_2$+γ (colonies), inter-crystalline γ grains, and BCC-B2 ($\beta_0$) phase fractions. The compressive strength at 700 °C was evaluated and strength of 566 MPa ± 23 for the DED and PBF was 465 MPa ± 49 was reported.

The two parts were fabricated as a feasibility study, as shown in Figure 14a DED and PBF processed γ-TiAl part (Fig. 14b) microstructure of DED repair atop a cast substrate. As can see from Figure 14a turbocharger wheel was fabricated via PBF, and a portion of the wheel was repaired (encircled region) successfully in the DED process. Figure 14b shows the transition microstructure of the cast substrate and DED built TNM-B1 alloy. A clear difference was observed between the larger grain size (lamellar grains) in as-cast and the smaller size in the DED zone. The smaller grain size is associated with the higher cooling rates in the DED process. The work demonstrates DED technology's viability for both fabrication and repair of turbine blades [22]. Boehm [131] has reported on the maintenance, repair and overhaul (MRO) of TiAl based turbine blades via a laser-based hybrid manufacturing system. In this case, the hybrid manufacturing system has a DED, 5-axes machining, in-process measurement, and milling provision. This work demonstrated the feasibility of repair of turbine components in adaptive and integrated approaches. The repair process starts with examination of the worn-out location of the turbine blade, which is then machined off via a milling operation. Then, the damage portion is rebuilt by adding the material in the machined location using DED. Finally, the rebuilt location is machined in the same system. Thus, laser-based hybrid manufacturing potentially reduces the repair time and cost [131].

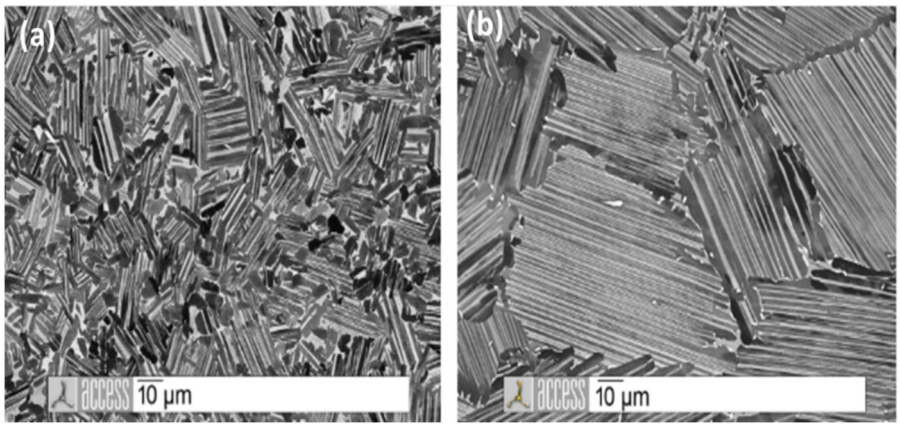


**Fig. 13.** Microstructure of the TNM alloy (a) In DED; and (b) In LPBF (Reproduced with the permission of Author/Publisher) [22].

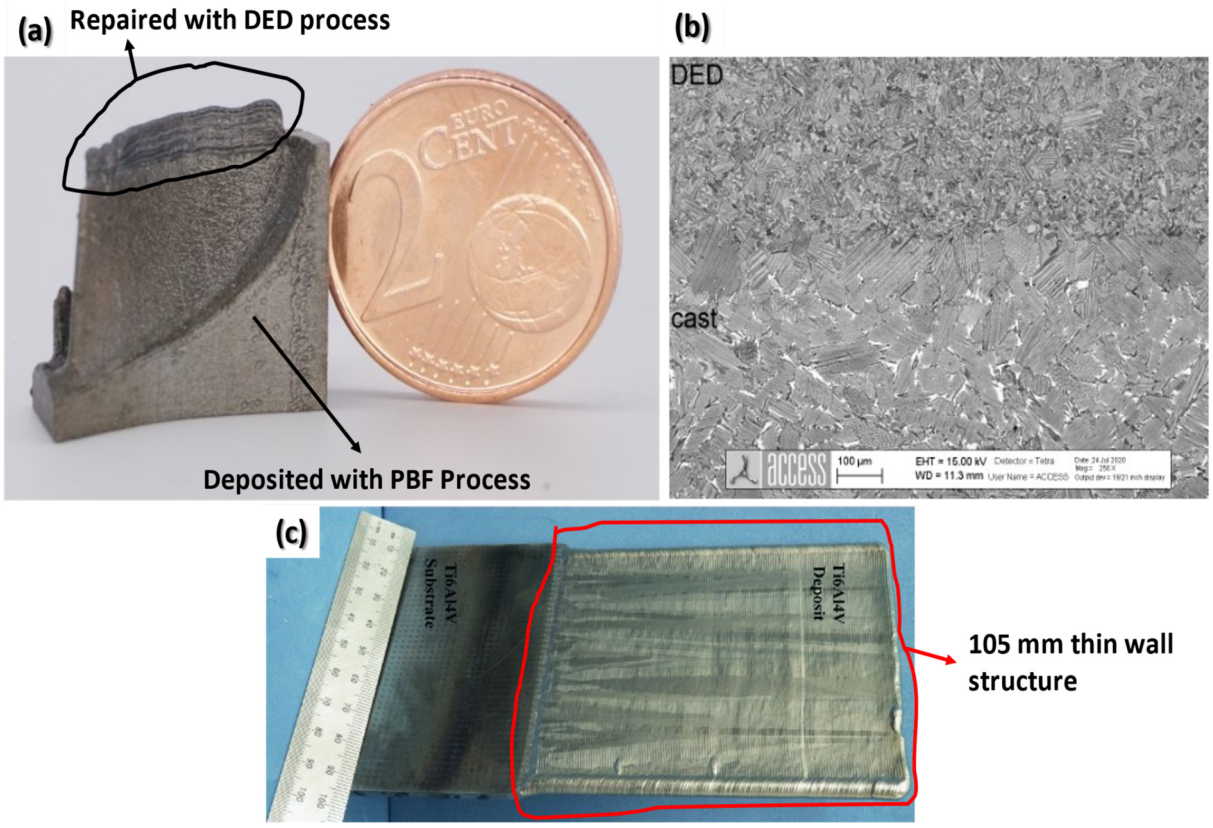


**Fig. 14.** γ-TiAl part (a) Built with PBF and repaired with the DED. (b) Microstructure of TiAl sample of the as-cast (base) and DED (top) material in heat-treated condition at 100×. (c) Thin wall structure deposited on 3 mm substrate/base plate (Reproduced with the permission of Author/Publisher) [22,134].

Ocylok et al. have reported that TiAl alloys are a front runner for replacing gas turbine blades due to weight-to-thrust ratio and service temperature up to 700 °C. As such, they conducted work to investigate DED TiAl based alloy for turbine blade repair applications. Before TiAl cladding, the substrate was preheated to 900 °C to reduce thermal stresses. The blades were then subjected to DED using a Ti-46.8Al-1Cr-0.2Si alloy with Si and TiB2. The addition of Si and TiB2 to the TiAl alloy enhanced the wear and corrosion properties of the clad [133]. In related work, Rittinghaus et al. 2020 [135] reported the possibility of TiAl component repair in DED. The TiAl alloy (GE4822) blade was built using the Laser Powder Bed Fusion (LPBF) process. The wheel portion was removed by machining and built back with the same material using the DED technique. The process conditions used during DED repair is presented in Table 7. This work demonstrates the hybrid manufacturing technique for the TiAl blade fabrication and repair.

Wanjara et al. [134] have reported on the WEBAM technique for repairing and refurbishing the fan blade leading

**Table 7.** Process conditions used to deposit the TiAl samples [135].

| Condition | Value |
|---|---|
| Laser power (W) | 66 |
| Beam diameter (mm) | 0.6 |
| Travel speed ($mm^{-s}$) | 8.33 |
| Powder flow rate ($g^{-s}$) | 0.025 |
| Hatch distance (mm) | 0.3 |
| Preheating (°C) | 900 |

edge of the Ti6Al4V alloy. For that 105 mm × 1 mm thin wall structure was fabricated on a 3 mm thick base plate, as shown in Figure 14c. The thin wall was inspected using X-Ray microcomputed tomography. Results indicate that no defects were found in the thin wall sample. Also, it was found that there was a low level of residual stress and distortion values. The investigation results encourage the repair and overhaul of the fan blade using the WEBAM process. Apart from the limited case studies discussed above, little work has been reported in the literature on repairing of the titanium aluminide components using DED. The available publications highlight that titanium aluminide is used in aero-engine parts due to its attractive properties, and that DED is a potential technology for repair of such components.

## 8 Challenges and opportunities

The contemporary TiAl-based alloy components are interested in aerospace and automotive parts for high-temperature applications. Several cases have shown the fabrication of TiAl components via casting, powder metallurgy, forging, and recently metal additive manufacturing. The metal additive manufacturing based directed energy deposition (DED) have problems to fabrication of defect-free parts due to steep temperature gradients, rapid cooling and remelting of previously deposited layers [73]. They induce thermal stress, cracks, delamination, inhomogeneous microstructure, and internal porosity. Hence one can work on the production of defect-free TiAl parts via DED technologies can be explored. Further, TiAl components used in high-temperature applications due to oxidation and fatigue lead to damage, wear out, and breakdowns. Replacing the entire part is not advisable as it is expensive. DED is a promising technique to produce, repair, rework, and overhaul damaged parts (MRO). The reclamation strategy is explored via potential DED techniques to add value to the high-cost TiAl components and enhance the life span of the TiAl components. Kimme and Rittinghaus have reported the potential of TiAl parts repair via DED [122,132]. Considering the high-quality standard of the aircraft industry, DED repaired TiAl parts to be certified for their future use in the aircraft is very important. However, no standards for the certification of TiAl repaired parts are reported. Researchers can address the issues involved in repairing, reworking, overhauling and certification of the components via DED.

## 9 Conclusion

A literature review on TiAl based alloys for aero-engine applications and the Directed Energy Deposition (DED) technique for the fabrication and reclamation of parts has been conducted. Observations are summarized below:

- TiAl alloys are starting to be used in aero engine parts due to their favourable intrinsic properties. TiAl has a high service temperature, high hardness and low density compared to conventional superalloys, thereby helping realize fuel savings that can lead to lower pollution.
- DED is a promising technique used to produce, repair, rework, and overhaul (MRO) damaged parts layer-by-layer. However, process parameters (laser power, travel speed, layer height, powder flow rate, preheat) need to be optimized to prevent cracking and ensure a suitable microstructure.
- Case studies reveal that DED is under consideration for repair of TiAl parts. Hybrid technology comprising machining, repair and finishing capability in a single machine is an attractive implementation strategy to improve repair efficiencies.
- The review shows that the investigations into development and applications of DED-based repairing techniques are limited, which suggests that further investigations are very much needed.

## Funding

This research work does not receive any financial assistance.

## Conflict of interest

The authors declare that they have no pecuniary or other personal interests influenced this research work.

## Author contributions

B. Mallikarjuna primarily contributed to the work conceptualization, collection of references, data curation, and original draft; E.W. Reutzel was involved in planning, and reviewing the manuscript.

## References

1. F. Appel, M. Paul, D.H. Oehring, Gamma titanium aluminide alloys: Science and technology, 1st ed. Wiley-VCH Verlag GmbH & Co. KGaA, 12, 69469 Weinheim, Germany, 2011
2. M. Balichakra, S. Bontha, P. Krishna, V.K. Balla, Prediction and validation of residual stresses generated during laser metal deposition of γ titanium aluminide thin wall structures, Mater. Res. Express. **6** (2019) 106550
3. J.C. Chesnutt, Titanium Aluminides for Aerospace Applications, in: D.L.K.S.D. Antolohch, R.W. Stusrud, R.A. Ma&Cay, D.L. Anton, T. Khan, R.D. Kissinger (Ed.), The Minerals, Metals & Materials Society, Ohio 1992, pp. 1–9.

4. J. Lapin, TiAl-based alloys: Present status and future perspectives, Metal. **19** (2009) 1–12
5. S.K. Rittinghaus, U. Hecht, V. Werner, A. Weisheit, Heat treatment of laser metal deposited TiAl TNM alloy, Intermetallics. **95** (2018) 94–101
6. K. Kothari, R. Radhakrishnan, N.M. Wereley, Advances in gamma titanium aluminides and their manufacturing techniques, Prog. Aerosp. Sci. **55** (2012) 1–16
7. P.A. Bartolotta, D.L. Krause, Titanium aluminide applications in the high speed civil transport, Gamma Titan. Alum. **1999** (1999) 3–10
8. W. Chen, Z. Li, Additive manufacturing of titanium aluminides, in: F. Froes, R. Boyer (Eds.), Addit. Manuf. Aerosp. Ind., Elsevier 2019, pp. 235–263
9. M. Dahms, Gamma titanium aluminide research and applications in germany and austria, Adv. Perform. Mater. **1** (1994) 157–182
10. G. Baudana, S. Biamino, D. Ugues, M. Lombardi, P. Fino, M. Pavese, C. Badini, Titanium aluminides for aerospace and automotive applications processed by electron beam melting: contribution of politecnico di torino, Met. Powder Rep. **74** (2016) 2–8
11. T. Tetsui, K. Shindo, S. Kobayashi, M. Takeyama, A newly developed hot worked TiAl alloy for blades and structural components, Scr. Mater. **47** (2002) 399–403
12. D. Pilone, G. Pulci, L. Paglia, A. Mondal, F. Marra, F. Felli, A. Brotzu, Mechanical behaviour of an $Al_2O_3$ dispersion strengthened γTiAl alloy produced by centrifugal casting, Metals (Basel). **10** (2020) 1–12
13. J. Aguilar, U. Hecht, A. Schievenbusch, Qualification of an investment casting process for production of titanium aluminide components for aerospace and automotive applications, Mater. Sci. Forum. **638–642** (2010) 1275–1280
14. T. Noda, Application of cast gamma TiAl for automobiles, Intermetallics. **6** (1998) 709–713
15. T. Tetsui, Development of a second generation TiAl turbocharger, Mater. Sci. Forum. **561–565** (2007) 379–382
16. T. Tetsui, Gamma Ti aluminides for non-aerospace applications, Curr. Opin. Solid State Mater. Sci. **4** (1999) 243–248
17. L.E. Murr, S.M. Gaytan, A. Ceylan, E. Martinez, J.L. Martinez, D.H. Hernandez, B.I. Machado, D.A. Ramirez, F. Medina, S. Collins, R.B. Wicker, Characterization of titanium aluminide alloy components fabricated by additive manufacturing using electron beam melting, Acta Mater. **58** (2009) 1887–1894
18. D. Chandley, P. Metal, Use of gamma titanium aluminide for automotive engine valves, Metall. Sci. Technol. Teksid. (2000) 8–11
19. W. Sheng, D. Li, R. Yang, Y. Liu, Research on the Ti-48Al-2Cr-2Nb automobile exhaust valve formed in permanent mold casting during centrifugal casting process, J. Mater. Sci. Techologyogy. **17** (2001) s97–s100
20. A. Pathania, S.A. Kumar, B.K. Nagesha, S. Barad, T.N. Suresh, Reclamation of titanium alloy based aerospace parts using laser based metal deposition methodology, Mater. Today Proc. **45** (2021) 4886–4892
21. J. Wang, S. Prakash, Y.V. Joshi, F. Liou, Laser aided part repair-A review, in: Solid Free. Fabr. Symp., 2002: p. na. https://www.semanticscholar.org/paper/Laser-Aided-Part-Repair-a-Review-Wang-Prakash/d3f64dd44856d73d13cdce54e83634b7f808e989#extracted.
22. S. Rittinghaus, J. Schmelzer, M.W. Rackel, S. Hemes, A. Vogelpoth, U. Hecht, A. Weisheit, Direct energy deposition of TiAl for hybrid manufacturing and repair of turbine blades, Materials (Basel). **13** (2020) 4392
23. M.K. Keshavarz, A. Gontcharov, P. Lowden, A. Chan, D. Kulkarni, M. Brochu, Turbine blade tip repair by laser directed energy deposition additive manufacturing using a Rene 142-MERL 72 powder blend, J. Manuf. Mater. Process. **5** (2021) 21
24. V.I. Chukwuike, O.G. Echem, S. Prabhakaran, S. Anandkumar, R.C. Barik, Laser shock peening (LSP): Electrochemical and hydrodynamic investigation of corrosion protection pre-treatment for a copper surface in 3.5% NaCl medium, Corros. Sci. **179** (2021) 109156
25. K.A. Ellison, P. Lowden, J. Liburdi, Powder metallurgy repair of turbine components, in: Int. Gas Turbine Aeroengine Congr. Expo., 1992, pp. 1–8
26. S. Nowotny, S. Scharek, E. Beyer, K. Richter, Laser beam build-up welding-Precision in repair, surface cladding, and direct 3D metal deposition, J. Therm. Spray Technol. **16** (2007) 344–348
27. B. Wu, J. Wang, Y. Zhang, M. Luo, Adaptive location of repaired blade for multi-axis milling, J. Comput. Des. Eng. **2** (2015) 261–267
28. Y.P.U. Kathuria, Some aspects of laser surface cladding in the turbine industry, Surf. Coat. Technol. **132** (2000) 262–269
29. K. Gupta, LASER cladding-A post processing technique for coating, repair and re-manufacturing, in: Mater. Forming, Mach. Post Process, Springer, Cham, 2019, pp. 231–249
30. L. Shepeleva, B. Medres, W.D. Kaplan, M. Bamberger, A. Weisheit, Laser cladding of turbine blades, Surf. Coat. Technol. **125** (2000) 45–48
31. M. Nicolaus, K. Mohwald, H.J. Maier, A combined brazing and aluminizing process for repairing turbine blades by thermal spraying using the coating system NiCrSi/NiCoCrAlY/Al, J. Therm. Spray Technol. **26** (2017) 1659–1668
32. M. Nicolaus, K. Möhwald, H.J. Maier, Thermally sprayed nickel-based repair coatings for high-pressure turbine blades: Controlling void formation during a combined brazing and aluminizing process, Coatings. **11** (2021) 725
33. L. GmbH, Laser cladding, Laserline. (2021) 1–6
34. A.I. Gorunov, Complex refurbishment of titanium turbine blades by applying heat-resistant coatings by direct metal deposition, Eng. Fail. Anal. **86** (2018) 115–130
35. Z. Xiong, G. Chen, X. Zeng, Effects of process variables on interfacial quality of laser cladding on aeroengine blade material GH4133, J. Mater. Process. Technol. **9** (2008) 930–936
36. I. Shishkovsky, I. Smurov, Titanium base functional graded coating via 3D laser cladding, Mater. Lett. **73** (2012) 32–35
37. S. Rittinghaus, J. Schmelzer, M.W. Rackel, S. Hemes, A. Vogelpoth, U. Hecht, A. Weisheit, Direct energy deposition of TiAl for hybrid manufacturing and repair of turbine blades, Materials (Basel). **13** (2020) 4392
38. M. Göbel, A. Gasser, K. Wissenbach, R. Poprawe, LMD process diagrams for blade tip repair, Laser Inst. Am. **1002** (2016) 1–10
39. S.M. Yusuf, S. Cutler, N. Gao, Review: the impact of metal additive manufacturing on the aerospace industry, Metals (Basel). **57** (2019) 779

40. M. Leino, J. Pekkarinen, R. Soukka, The role of laser additive manufacturing methods of metals in repair, refurbishment and remanufacturing-enabling circular economy, in: 9th Int. Conf. Photonic Technol. 2016, 2016: pp. 752–760
41. S. Inc., Metal 3D printing applications & industries, Sciaky's Inc. (2021), pp. 1–8. https://www.sciaky.com/additive-manufacturing/applications-industries
42. G. Thomas, Additive manufacturing: opportunities and constraints, 2013. https://www.raeng.org.uk/publications/reports/additive-manufacturing
43. N. Jayanth, P. Senthil, B. Mallikarjuna, Experimental investigation on the application of FDM 3D printed conductive ABS-CB composite in EMI shielding, Radiat. Phys. Chem. **198** (2022) 110263
44. B. Mallikarjuna, K. Jayachristiyan, Innovative modeling and rapid prototyping of turbocharger impeller, in: Int. Conf. Adv. Mater. Manuf. Manag. Therm. Sci., 2013, pp. 1426–1432
45. N. Jayanth, K. Jaswanthraj, S. Sandeep, N.H. Mallaya, S.R. Siddharth, Effect of heat treatment on mechanical properties of 3D printed PLA, J. Mech. Behav. Biomed. Mater. **123** (2021) 104764
46. Z. Yan, W. Liu, Z. Tang, X. Liu, N. Zhang, M. Li, H. Zhang, Review on thermal analysis in laser-based additive manufacturing, Opt. Laser Technol. **106** (2018) 427–441
47. A.H. Azman, Additive manufacturing for repair and restoration in remanufacturing: An overview from object design and systems perspectives, Processes **7** (2019) 802
48. A. Saboori, A. Aversa, G. Marchese, S. Biamino, Application of directed energy deposition-based additive manufacturing in repair, Appl. Sci. **9** (2019) 3316
49. A. Saboori, D. Gallo, S. Biamino, P. Fino, M. Lombardi, An overview of additive manufacturing of titanium components by directed energy deposition: microstructure and mechanical properties, Appl. Sci. **7** (2017) 883
50. S. Alya, C. Vundru, B. Ankamreddy, R. Singh, Modeling of deposition geometry in laser directed energy deposition over inclined surfaces for restoration and remanufacturing, Trans. Indian Natl. Acad. Eng. (2021)
51. P. Leo, G. Renna, G. Casalino, Study of the direct metal deposition of AA2024 by electro spark for coating and reparation scopes, Appl. Sci. **7** (2017) 945
52. S. Thompson, Handbook of mould, tool and die repair welding, 1999. https://www.elsevier.com/books/handbook-of-mould-tool-and-die-repair-welding/thompson/978-1-85573-429-6
53. I. Nuclear, Robotic laser welding system improves steam generator repair, Int. At. Energy Agency. **21** (1990) 36–38
54. Z. Gui, A robot for welding repair of hydraulic turbine blade, in: IEEE Conf. Robot. Autom. Mechatronics, 2008, pp. 155–159
55. Z. Gui, Q. Chen, W. Zhang, Z. Sun, On-site rail-free robot for welding repair of turbine blade, in: 4th Korean-Sino Conf. Adv. Manuf. Technol., 2014, pp. 74–76
56. A.J. Pinkerton, W. Wang, L. Li, Component repair using laser direct metal deposition, Proc. Inst. Mech. Eng. Part B **222** (2008) 827–836
57. M. Balichakra, S. Bontha, P. Krishna, V.K. Balla, Laser surface melting of γ-TiAl alloy an experimental and numerical modeling study, Mater. Res. Express. **6** (2019) 046543
58. R. Liu, Z. Wang, T. Sparks, F. Liou, J. Newkirk, Aerospace applications of laser additive manufacturing, in: M. Brandt (Ed.), Laser Addit. Manuf., Woodhead Publishing, 2017, pp. 351–371
59. J.L. and D.G. Waugh, Laser surface engineering process and applications (2015)
60. G. Baudana, S. Biamino, B. Kloden, A. Kirchner, T. Weißgarber, B. Kieback, M. Pavese, D. Ugues, P. Fino, C. Badini, Electron beam melting of Ti-48Al-2Nb-0.7Cr-0.3Si: feasibility investigation, Intermetallics **73** (2016) 43–49
61. B. Mallikarjuna, S. Bontha, P. Krishna, V.K. Balla, Characterization and thermal analysis of laser metal deposited γ-TiAl thin walls, J. Mater. Res. Technol. **15** (2021) 6231–6243
62. G.E. Additive, New manufacturing milestone: 30,000 additive fuel nozzles, GE Addit. (2021) 1–4
63. S. Rittinghaus, J. Zielinski, Influence of process conditions on the local solidification and microstructure during laser metal deposition of an intermetallic TiAl alloy (GE4822), Metall. Mater. Trans. A. **52** (2021) 1106–1116
64. J. Wang, Z. Pan, Y. Ma, Y. Lu, C. Shen, D. Cuiuri, H. Li, Characterization of wire arc additively manufactured titanium aluminide functionally graded material: Microstructure, mechanical properties and oxidation behaviour, Mater. Sci. Eng. A. **734** (2018) 110–119
65. P. Gao, W. Huang, H. Yang, G. Jing, Q. Liu, G. Wang, Z. Wang, X. Zeng, Cracking behavior and control of β-solidifying Ti-40Al-9V-0.5Y alloy produced by selective laser melting, J. Mater. Sci. Technol. **39** (2020) 144–154
66. D. Srivastava, Microstructural characterization of the γ-TiAl alloy samples fabricated by direct laser fabrication rapid prototype technique, Bull. Mater. Sci. **25** (2002) 619–633
67. V. Güther, M. Allen, J. Klose, H. Clemens, Metallurgical processing of titanium aluminides on industrial scale, Intermetallics. **103** (2018) 12–22
68. B.P. Bewlay, S. Nag, A. Suzuki, M.J. Weimer, TiAl alloys in commercial aircraft engines, Mater. High Temp. **33** (2016) 549–559
69. X.D. Zhang, C. Brice, D.W. Mahaffey, H. Zhang, K. Schwendner, D.J. Evans, H.L. Fraser, Characterization of laser-deposited TiAl alloys, Scr. Mater. **44** (2001) 2419–2424
70. M. Thomas, T. Malot, P. Aubry, C. Colin, T. Vilaro, P. Bertrand, The prospects for additive manufacturing of bulk TiAl alloy, Mater. High Temp. **33** (2016) 571–577
71. W. Liu, J.N. Dupont, Fabrication of carbide-particle-reinforced titanium aluminide-matrix composites by laser-engineered net shaping, Metall. Mater. Trans. A Phys. Metall. Mater. Sci. **35** (2004) 1133–1140
72. V.K. Balla, M. Das, A. Mohammad, A.M. Al-ahmari, Additive manufacturing of g −TiAl: processing, microstructure, and properties, Adv. Eng. Eater. **18** (2016) 1–8
73. C. Li, Z.Y. Liu, X.Y. Fang, Y.B. Guo, Residual stress in metal additive manufacturing, in: Procedia CIRP, 2018, pp. 348–353
74. P. Rangaswamy, M.L. Griffith, M.B. Prime, T.M. Holden, R.B. Rogge, J.M. Edwards, R.J. Sebring, Residual stresses in LENS® components using neutron diffraction and contour method, Mater. Sci. Eng. A. **399** (2005) 72–83
75. M. Balichakra, S. Bontha, P. Krishna, M. Das, V.K. Balla, Understanding thermal behavior in laser processing of titanium aluminide alloys, in: Proc. 6th Int. 27th All India Manuf. Technol. Des. Res. Conf., 2016, pp. 73–77

76. W. Chen, Z. Li, Additive manufacturing of titanium aluminides, Elsevier, 2019, pp. 235–263
77. H.P. Tang, G.Y. Yang, W.P. Jia, W.W. He, S.L. Lu, M. Qian, Additive manufacturing of a high niobium-containing titanium aluminide alloy by selective electron beam melting, Mater. Sci. Eng. A. **636** (2015) 103–107
78. B. Kemerling, J.C. Lippold, C.M. Fancher, J. Bunn, Residual stress evaluation of components produced via direct metal laser sintering, Weld. World. (2018)
79. H.A. Soliman, M. Elbestawi, Titanium aluminides processing by additive manufacturing – a review, Springer, London, 2022
80. F.M. Abdullah, S. Anwar, Thermomechanical simulations of residual stresses and distortion in electron beam melting with experimental validation for Ti-6Al-4V, Metals (Basel). **10** (2020) 1151
81. S. Lee, J. Kim, J. Choe, S.W. Kim, J.K. Hong, Y.S. Choi, Understanding crack formation mechanisms of Ti-48Al-2Cr-2Nb single tracks during laser powder bed fusion, Met. Mater. Int. **27** (2021) 78–91
82. E. Mirkoohi, D.E. Seivers, H. Garmestani, S.Y. Liang, Heat source modeling in selective laser melting, Materials (Basel). **12** (2019) 1–18
83. R.M. Mahamood, E.T. Akinlabi, Effect of laser power on surface finish during laser metal deposition process, 2014, pp. 965–969
84. A. Martín, C.M. Cepeda-Jiménez, M.T. Pérez-Prado, Gas atomization of γ-TiAl alloy powder for additive manufacturing, Adv. Eng. Mater. **22** (2020)
85. H.P. Qu, P. Li, S.Q. Zhang, A. Li, H.M. Wang, The effects of heat treatment on the microstructure and mechanical property of laser melting deposition γ-TiAl intermetallic alloys, Mater. Des. **31** (2009) 2201–2210
86. M. Thomas, T. Malot, P. Aubry, Laser metal deposition of the intermetallic TiAl alloy, Metall. Mater. Trans. A. **48** (2017) 1–16
87. K.O. Abdulrahman, E.T. Akinlabi, R.M. Mahamood, Characteristics of laser metal deposited titanium aluminide, Mater. Res. Express Pap. **6** (2019) 046504
88. M. Tlotleng, Microstructural properties of heat-treated LENS in situ additively manufactured titanium aluminide, J. Mater. Eng. Perform. **28** (2018) 701–708
89. M. Tlotleng, S. Pityana, LENS manufactured γ-TNB turbine blade using Laser "in situ" alloying approach, MRS Adv. **5** (2020) 1203–1213
90. Z. Liu, C. Wang, W. Wang, G. Xu, X. Liu, Effects of Tantalum on the microstructure and properties of Ti-48Al-2Cr-2Nb alloy fabricated via laser additive manufacturing, Mater. Charact. **179** (2021) 111317
91. H. Chen, Z. Liu, X. Cheng, Y. Zou, Laser deposition of graded γ-TiAl-Ti2AlNb alloys- Microstructure and nanomechanical characterization of the transition zone.pdf, J. Alloys Compd. **875** (2021) 159946
92. D. Huang, Q. Tan, Y. Zhou, Y. Yi, F. Wang, T. Wu, X. Yang, Z. Fan, Y. Liu, J. Zhang, H. Huang, M. Yan, M.-X. Zhang, The significant impact of grain refiner on γ-TiAl intermetallic fabricated by laser-based additive manufacturing, Addit. Manuf. **46** (2021) 102172
93. J. Xu, Q. Zhou, J. Kong, Y. Peng, S. Guo, J. Zhu, J. Fan, Solidification behavior and microstructure of Ti-(37−52) at% Al alloys synthesized in situ via dual-wire electron beam freeform fabrication, Addit. Manuf. **46** (2021)
94. V.R. Utyaganova, K.N. Kalashnikov, D.A. Gurianov, Microstructure and microhardness of wire-feed electron-beam additive manufactured Ti-Al thin-walled elements, in: AIP Conf. Proc., 2019, p. 020377
95. M. Yan, F. Yang, B. Lu, C. Chen, Y. Sui, Z. Guo, Microstructure and mechanical properties of high relative density γ-TiAl alloy using irregular pre-alloyed powder, Metals (Basel). **11** (2021) 635
96. M. Griffith, M. Schlienger, L. Harwell, M. Oliver, M. Baldwin, M. Ensz, M. Essien, J. Brooks, C. Robino, J. Smugeresky, W. Hofmeister, M. Wert, D. Nelson, Understanding thermal behavior in the LENS process, Mater. Des. **20** (1999) 107–113
97. S. Bontha, The effect of process variables on microstructure in Laser Deposited Materials, Wright State University, 2006
98. E. Foroozmehr, R. Kovacevic, Effect of path planning on the laser powder deposition process: Thermal and structural evaluation, Int. J. Adv. Manuf. Technol. **51** (2010) 659–669
99. Z. Luo, Y. Zhao, A survey of finite element analysis of temperature and thermal stress fields in powder bed fusion additive manufacturing, Addit. Manuf. **21** (2018) 318–332
100. B. Hazarika, B. Mallikarjuna, P. Krishna, V.K. Balla, S. Bontha, Numerical modelling of laser additive manufacturing processes, in: NAFEMS India Reg. Conf., 2016, pp. 30–31
101. I.A. Roberts, C.J. Wang, M. Stanford, K.A. Kibble, D.J. Mynors, Experimental and numerical analysis of residual stresses in additive layer manufacturing by laser melting of metal powders, Key Eng. Mater. **450** (2011) 461–465
102. X. Zhou, H. Zhang, G. Wang, X. Bai, Three-dimensional numerical simulation of arc and metal transport in arc welding based additive manufacturing, Int. J. Heat Mass Transf. **103** (2016) 521–537
103. M.L. Hupert, M.A. Witek, Y. Wang, M.W. Mitchell, X. Liu, Y. Bejat, D.E. Nikitopoulos, J. Goettert, M.C. Murphy, S.A. Soper, Polymer-based microfluidic devices for biomedical applications, Microfluid. BioMEMS, Med. Microsyst. **4982** (2003) 52–64
104. T. Mukherjee, V. Manvatkar, T. Debroy, Mitigation of thermal distortion during additive manufacturing, Scr. Mater. **127** (2017) 79–83
105. T. Amine, J.W. Newkirk, F. Liou, An investigation of the effect of direct metal deposition parameters on the characteristics of the deposited layers, Case Stud. Therm. Eng. **3** (2014) 21–34
106. A. Soleymani, Thermal model for prediction of deposition dimension of a deposited nickel superalloy, Int. J. Eng. Adv. Technol. **4** (2015) 191–196
107. A.M. Kamara, S. Marimuthu, L. Li, A numerical investigation into residual stress characteristics in laser deposited multiple layer waspaloy parts, J. Manuf. Sci. Eng. **133** (2011) 031013
108. N.C. Levkulich, S.L. Semiatin, J.E. Gockel, J.R. Middendorf, A.T. DeWald, N.W. Klingbeil, The effect of process parameters on residual stress evolution and distortion in the laser powder bed fusion of Ti-6Al-4V, Addit. Manuf. **28** (2019) 475–484
109. I.A. Roberts, C.J. Wang, R. Esterlein, M. Stanford, D.J. Mynors, A three-dimensional finite element analysis of the temperature field during laser melting of metal powders in additive layer manufacturing, Int. J. Mach. Tools Manuf. **49** (2009) 916–923

110. L. Wang, S. Felicelli, Y. Gooroochurn, P.T. Wang, M.F. Horstemeyer, Optimization of the LENS® process for steady molten pool size, Mater. Sci. Eng. A **474** (2008) 148–156
111. S. Marimuthu, D. Clark, J. Allen, A.M. Kamara, P. Mativenga, L. Li, R. Scudamore, Finite element modelling of substrate thermal distortion in direct laser additive manufacture of an aero-engine component, Proc. Inst. Mech. Eng. Part C J. Mech. Eng. Sci. **227** (2013) 1987–1999
112. T. Mukherjee, J.S. Zuback, W. Zhang, T. Debroy, Residual stresses and distortion in additively manufactured compositionally graded and dissimilar joints, Comput. Mater. Sci. **143** (2017) 325–337
113. B. Ahmad, S.V.D.V. Veen, M.E. Fitzpatrick, H. Guo, Measurement and modelling of residual stress in wire-feed additively manufactured titanium, Mater. Sci. Technol. **34** (2018) 2250–2259
114. X. Lu, M. Chiumenti, M. Cervera, J. Li, X. Lin, L. Ma, G. Zhang, E. Liang, Substrate design to minimize residual stresses in Directed Energy Deposition AM processes, Mater. Des. **202** (2021) 109525
115. S. Zekovic, R. Dwivedi, R. Kovacevic, Thermo-structural finite element analysis of direct laser metal deposited thin-walled structures, in: Solid Free. Fabr., 2005, pp. 338–355
116. H. Jing, P. Ge, Z. Zhang, J.Q. Chen, Z.M. Liu, W.W. Liu, Numerical studies of the effects of the substrate structure on the residual stress in laser directed energy additive manufacturing of thin-walled products, Metals (Basel). **12** (2022)
117. F. Sikan, P. Wanjara, J. Gholipour, A. Kumar, M. Brochu, Thermo-mechanical modeling of wire-fed electron beam additive manufacturing, Materials (Basel). **14** (2021) 1–21
118. L. Yan, W. Li, X. Chen, Y. Zhang, J. Newkirk, F. Liou, D. Dietrich, Simulation of cooling rate effects on Ti-48Al-2Cr-2Nb crack formation in direct laser deposition, in: Proc. 27th Annu. Int. Solid Free. Fabr. Symp. Addit. Manuf. Conf., 2016, pp. 680–690
119. J. Wang, H. Wang, X. Cheng, B. Zhang, Y. Wu, S. Zhang, X. Tian, Prediction of solidification microstructure of titanium aluminum intermetallic alloy by laser surface remelting, Opt. Laser Technol. **147** (2022)
120. F. Caiazzo, V. Alfieri, Simulation of laser-assisted directed energy deposition of aluminum powder: prediction of geometry and temperature evolution, Materials (Basel). **12** (2019)
121. F. Caiazzo, V. Alfieri, G. Bolelli, Residual stress in laser-based directed energy deposition of aluminum alloy 2024: simulation and validation, Int. J. Adv. Manuf. Technol. **118** (2022) 1197–1211
122. T. Kimme, M. Seifert, Laser surface cladding of titanium aluminides, Laser Tech. J. (2017) 18–20
123. M. Rauch, J.-Y. Hascoët, M. Mallaiah, Repairing Ti-6Al-4V aeronautical components with DED additive manufacturing, in: MATEC Web Conf., 2020, p. 03017
124. J.M. Wilson, C. Piya, Y.C. Shin, F. Zhao, K. Ramani, Remanufacturing of turbine blades by laser direct deposition with its energy and environmental impact analysis, J. Clean. Prod. **80** (2014) 170–178
125. B. Carcel, A. Serrano, J. Zambrano, V. Amigo, A.C. Carcel, Laser cladding of TiAl intermetallic alloy on Ti6Al4V process optimization and properties, Phys. Proc. **56** (2014) 284–293
126. Z.F. Li, G.Q. Wu, Z. Huang, Z.J. Ruan, Diffusion bonding of laser surface modified TiAl alloy/Ni alloy, Mater. Lett. **58** (2004) 3470–3473
127. G.X. Luo, G.Q. Wu, Z. Huang, Z.J. Ruan, Diffusion bonding of laser-surface-modified gamma titanium aluminide alloy to nickel-base casting alloy, Scr. Mater. **57** (2007) 521–524
128. M. Balichakra, S. Bontha, P. Krishna, M. Das, V.K. Balla, Understanding thermal behavior in laser processing of titanium aluminide alloys, in: Proc. 6th Int. 27th All India Manuf. Technol. Des. Res. Conf., 2016, pp. 73–77.
129. K. Kothari, R. Radhakrishnan, N.M. Wereley, Characterization of rapidly consolidated titanium diboride, J. Eng. Mater. Technol. **133** (2011) 024501
130. M. Thomas, T. Malot, P. Aubry, C. Colin, T. Vilaro, P. Bertrand, The prospects for additive manufacturing of bulk TiAl alloy, Mater. High Temp. **33** (2016) 571–577
131. V. Boehm, Hybrid manufacturing of turbine components, Laser Tech. J. **13** (2016) 44–47
132. S. Rittinghaus, Va. Weishei, M. Mathes, W.G. Vargas, Laser metal deposition of titanium aluminides-A future repair technology for jet engine blades?, in: Proc. 13th World Conf. Titan., 2016, pp. 1205–1210
133. S. Ocylok, A. Weisheit, I. Kelbassa, Increased wear and oxidation resistance of titanium aluminide alloys by laser cladding, Adv. Mater. Res. **278** (2011) 515–520
134. P. Wanjara, K. Watanabe, C. De Formanoir, Q. Yang, C. Bescond, S. Godet, M. Brochu, K. Nezaki, J. Gholipour, P. Patnaik, Titanium alloy repair with wire-feed electron beam additive manufacturing technology, Adv. Mater. Sci. Eng. **2019** (2019) 23
135. S. Rittinghaus, V. Rocio, M. Ramirez, A. Vogelpoth, U. Hecht, J. Schmelzer, Laser based manufacturing of titanium aluminides, in: 14th World Conf. Titan., 2020, p. 08001


**Cite this article as**: Balichakra Mallikarjuna, Edward W. Reutzel, Reclamation of intermetallic titanium aluminide aero-engine components using directed energy deposition technology, Manufacturing Rev. **9**, 27 (2022)